

Table of Contents:

Abstract.....	3
Introduction.....	3
Dynamic Force Analysis of the Mechanism.....	3-9
Free Body Diagram and Equations.....	3-8
Appropriate Hydraulic Actuator.....	8
Method of Inspection when $R_{22} = 100\text{mm}$	9-10
Static Force Analysis of the Mechanism – Analytical Method.....	11-16
Free Body Diagram and Equations.....	11
Method of Inspection when $R_{22} = 100\text{mm}$	13-14
Static Force Analysis Plots.....	15-16
Static Force Analysis of the Mechanism – Graphical Method.....	16-22
Type of Member.....	16
Iteration #1.....	16-17
Iteration #2.....	18-19
Iteration #3.....	19-21
Iteration Comparison.....	21
Analytical and Graphical Comparison.....	22
The Equation of Motion.....	22-25
Equivalent Mass Moment of Inertia.....	22-23
Change in Kinetic Energy.....	23-24
Change in Potential Energy.....	24
Change in Work due to External Forces.....	24
Power Equation.....	25
Percent Contribution.....	25
Tangential Component of F_p	25
Conclusion.....	25
Appendix.....	26-31
Appendix A – Dynamic Force Analysis.....	26-28
Appendix B – Static Force Analysis.....	29-31
Appendix C – Equation of Motion.....	31

Abstract:

This assignment is intended to teach more about a particular system that is already very well known. In the following report, force analysis of the mechanism in Figure.1 will be completed both dynamically and statically (in Analytical, Graphical, and with the Equation of Motion) in a symbolic manner, and for a particular instant ($R_{22} = 100$ mm).

Introduction:

In this mechanism a wheel is being pushed by hydraulic actuator (link 9) away from a joint O_4 , and the wheel center moves from 75 mm from O_4 to 150 mm from O_4 . There is also a spring (link 8) that appears in the same plane as the actuator connecting the center of mass of link 2 to ground at O_8 .

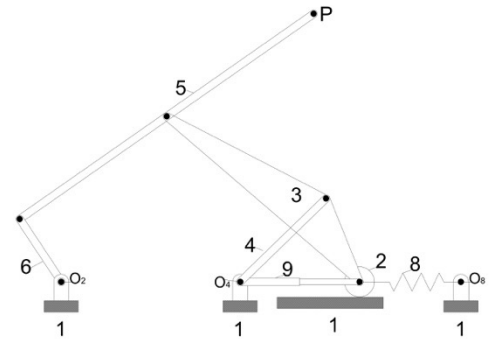


Figure 1: Mechanism to be Analyzed

I: Dynamic Force Analysis of the Mechanism

To determine the internal reaction forces between all of the links, each link has to be drawn as a free body diagram with the X and Y components of each force separate. In addition to drawing these free body diagrams, each link will include three equations that will assist in solving for the internal reaction forces; a sum of the forces in the X direction (ΣF_x), a sum of the forces in the Y direction (ΣF_y), and the sum of the moments about a particular point (ΣM). Particular links may have additional equations to assist in calculating the solution, but every single link will have the three basic force equations ($\Sigma F_x/\Sigma F_y/\Sigma M$). The following few statements will describe the exact process used to determine the internal reaction forces for all of the links in this system, in addition to providing plots of each link’s reaction force over the course of the move.

The first link to be analyzed is the hydraulic actuator where the unknowns without any analysis completed are F_{19X} , F_{19Y} , F_{29X} , and F_{29Y} . The free body diagram (Figure.2) and symbolic force equations can be seen below.

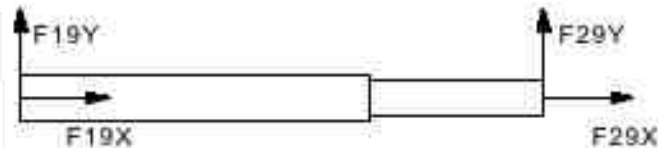


Figure 2 Free Body Diagram of Link 9

$$\Sigma F_x = F_{19X} + F_{29X} = m_9 A_{G9X} = 0 \text{ (Eqn. a)}$$

$$\Sigma F_y = F_{19Y} + F_{29Y} = m_9 A_{G9Y} = 0 \text{ (Eqn. b)}$$

$$\Sigma M_{O19} = R_{9X} * F_{29Y} = I_9 \alpha_9 = 0 \text{ (Eqn. c)}$$

The actuator force (F_{19X}) can also be described by the equation $F_{19X} = C * (R_{22} \dot{\quad})$ (Eqn. d).

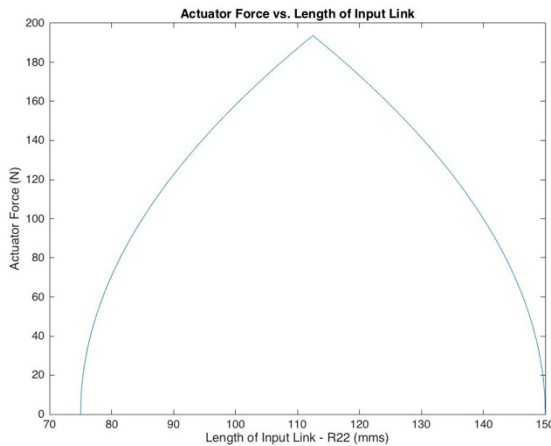


Figure 3 F_{19X} - Actuator Force

Using Eqn. d, F_{19X} is calculated and because there is no acceleration in the linear actuator, Eqn. a is used to determine that $F_{29X} = - F_{19X}$. The tabulated data for F_{19X} can be found in Appendix A.1, and the plot of F_{19X} over the course of the move is seen to the side in Figure.3. As expected, the actuator force increases when R_{22} accelerates, and decreases when R_{22} decelerates. The specific profile of the force is due to the velocity change over time.

Using Eqn. c, and including the information that the actuator does not have an angular acceleration, it must be determined that $F_{29y} = 0$, because the actuator must have a value for R_{9x} as that is a basic component of it being an actuator. Finally, Eqn. b determines that $F_{19y} = -F_{29y}$ which means that F_{19y} must also equal zero.

The next link to be analyzed is the spring. The original unknowns are F_{18x} , F_{18y} , F_{28x} , and F_{28y} . The free body diagram (Figure.4) and symbolic force equations can be seen below.

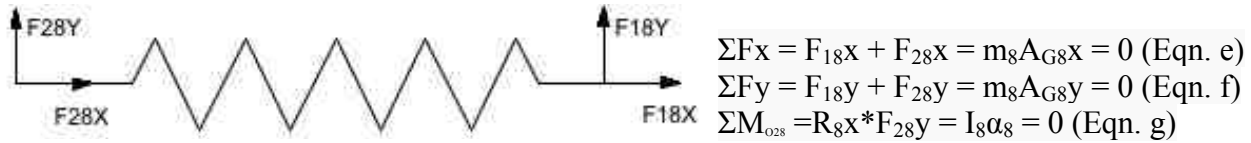


Figure 4 Free Body Diagram of Link 8

The spring force (F_{18x}) can also be described by the equation $F_{18x} = k*(R_{11}-R_{22}-R_s)$ (Eqn. h).

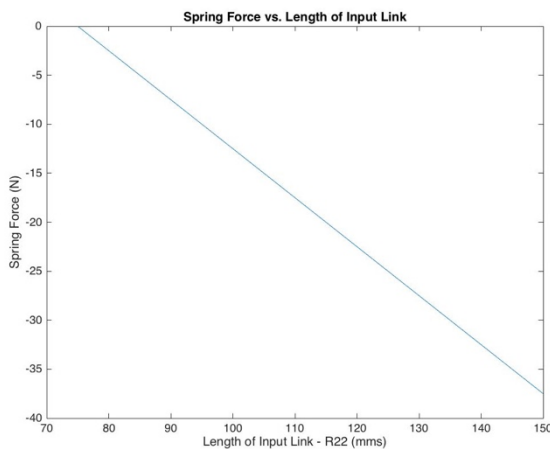


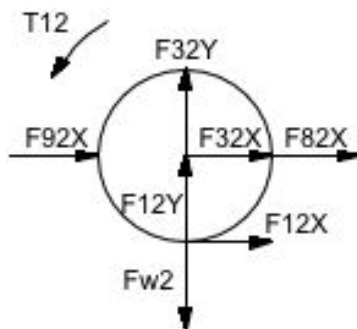
Figure 5 F_{18x} -Spring Force

the spring force is solely reliant on the change in value R_{22} , so as R_{22} increases from 75 mm to 150 mm, the spring force will decrease linearly.

By using Eqn. h, F_{18x} is calculated, and because there is no acceleration in the spring, Eqn. e is used to determine that $F_{28x} = -F_{18x}$. By using Eqn. g, and including the information that the spring does not have an angular acceleration, it must be determined that $F_{28y} = 0$, because the spring must have a value for R_{8x} (a length) for it to be a spring. Finally, Eqn. f determines that $F_{18y} = -F_{28y}$ which means that F_{18y} must also equal zero.

The tabulated data for F_{18x} (the spring force) can be found in Appendix A.1, and the plot of the spring force can be seen above in Figure.5. As can be seen,

Link 2 is the next link to be analyzed, and the original unknowns of this link are F_{12x} , F_{12y} , F_{32x} , and F_{32y} . The free body diagram (Figure.6) and symbolic force equations can be seen below.



$$\Sigma F_x = F_{92x} + F_{32x} + F_{82x} + F_{12x} = m_2 A_{G2x} \text{ (Eqn. 1)}$$

$$\Sigma F_y = F_{32y} + F_{12y} - F_{w2} = m_2 A_{G2y} = 0 \text{ (Eqn. 2)}$$

$$\Sigma M_{G2} = T_2 + \rho * F_{12x} = I_{G2} \alpha_2 \text{ (Eqn. 3)}$$

There is also a relationship between F_{12y} and F_{12x} that will assist in solving for the internal reaction forces of this link:

$$F_{12y} = \text{abs}(F_{12x}/\mu) \text{ (Eqn. 4)}$$

F_{12x} can be calculated by manipulating Eqn. 3, and then F_{12y} can be calculated using Eqn. 4 after that. The additional two unknowns (F_{32x} and F_{32y}) can be calculated using Eqns 1 and 2 using the

knowledge that $F_{92x} = -F_{29x}$, $F_{82x} = -F_{28x}$, the acceleration of link 2 in the X direction is the input acceleration, and the acceleration of link 2 in the Y direction is zero. The tabulated values for

Figure 6 Free Body Diagram of Link 2

F_{12x} , F_{12y} , F_{32x} , and F_{32y} can be found in Appendix A.2, and the plotted components of F_{12} and F_{32} can be found below in Figure.7 and Figure.8 respectively.

By looking at Figure.7 it is evident to see that the normal force (F_{12y}) stays almost constant over

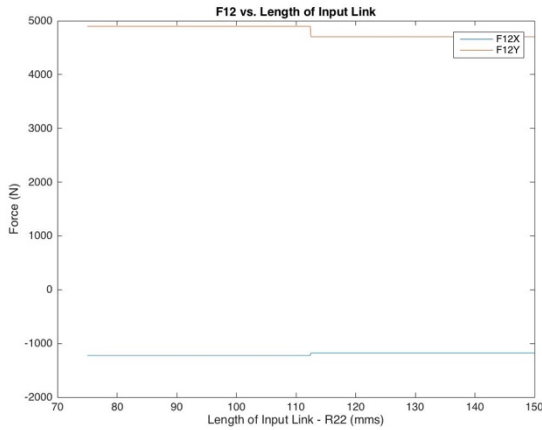


Figure 8 F_{12X} and F_{12Y}

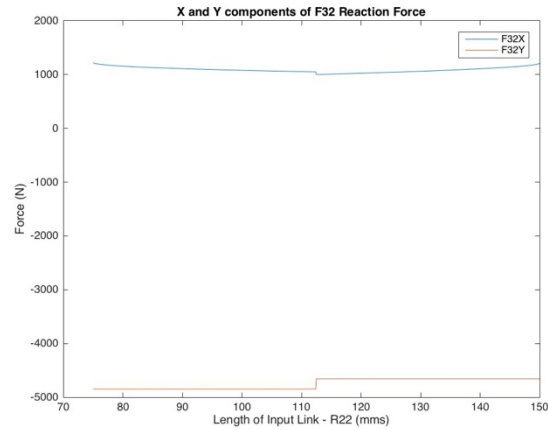


Figure 7 F_{32X} and F_{32Y}

the course of the move with an exception at $R_{22} = 110$ mms where the force drops a little due to a change in acceleration direction. The frictional force (F_{12x}), which depends on the normal force, also stays relatively constant over the course of the move. Figure.8 shows that F_{32x} and F_{32y} are also almost horizontal plots as they are affected mainly by F_{12x} and F_{12y} .

Link 3 is a bit more complicated to solve, so it will be solved in conjunction with link 4. The original unknowns for link 3 are F_{43x} , F_{43y} , F_{53x} , and F_{53y} , and the original unknowns for link 4 are F_{34x} , F_{34y} , F_{14x} , and F_{14y} . The free body diagrams (Link 3 = Figure.9, Link 4 = Figure.9a) and symbolic equations for both links can be seen below.

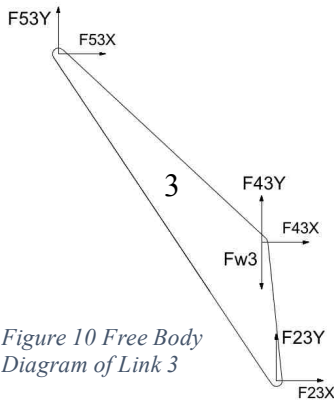


Figure 10 Free Body Diagram of Link 3

$$\begin{aligned} \Sigma F_x &= F_{53x} + F_{43x} + F_{23x} = m_3 A_{G3x} \text{ (Eqn. 5)} \\ \Sigma F_y &= F_{53y} + F_{43y} + F_{23y} - F_{w3} = m_3 A_{G3y} \text{ (Eqn. 6)} \\ \Sigma M_{O53} &= R_{333x} * F_{43y} - R_{333y} * F_{43x} - R_{333x} * g * m_3 - \\ & (R_{333x} * F_{23y} - R_{333y} * F_{23x}) = I_{G3} \alpha_3 + \\ & m_3 * (R_{333x} * A_{G3y} - R_{333y} * A_{G3x}) \text{ (Eqn. 7)} \end{aligned}$$

$$\begin{aligned} \Sigma F_x &= F_{14x} + F_{34x} = m_4 A_{G4x} = 0 \text{ (Eqn. 8)} \\ \Sigma F_y &= F_{14y} + F_{34y} - F_{w4} = m_4 A_{G4y} = 0 \text{ (Eqn. 9)} \\ \Sigma M_{G4} &= R_{4x} * F_{34y} - R_{4y} * F_{34x} = I_{G4} \alpha_4 \text{ (Eqn. 10)} \end{aligned}$$

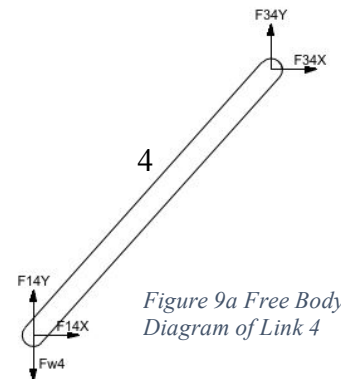


Figure 9a Free Body Diagram of Link 4

Eqn. 7 can be reorganized so that all values but those related to F_{43} be on the right side of the equal sign, and the F_{43} values are transformed into F_{34} values as $F_{34} = -F_{43}$. The resulting equation is as follows:

$$R_{333y} * F_{34x} - R_{333x} * F_{34y} = I_{G3} \alpha_3 + m_3 * (R_{333x} * A_{G3y} - R_{333y} * A_{G3x}) + R_{333x} * g * m_3 + (R_{333x} * F_{23y} - R_{333y} * F_{23x}) \text{ (Eqn. 7a)}$$

Similarly, Eqn. 10 can be reorganized so that all values but those related to F_{34} be on the right side of the equal sign. The resulting equation is as follows:

$$-R_{4y} * F_{34x} + R_{4x} * F_{34y} = I_{G4} \alpha_4 \text{ (Eqn. 10a)}$$

These two equations can thus be re-represented in a series of matrices as shown below:

$$\begin{bmatrix} R333y & -R333x \\ -R4y & R4x \end{bmatrix} \begin{bmatrix} F34x \\ F34y \end{bmatrix} = \begin{bmatrix} IG3\alpha_3 + m_3 * R333x * AG3y - m_3 * R333y * AG3x + R333x * g * m_3 + R33x * F23y - R33y * F23x \\ IG4\alpha_4 \end{bmatrix}$$

F_{34x} and F_{34y} can then be solved using Cramer's rule.

After this process is completed, Eqns 5 and 6 can be used to find F_{53x} and F_{53y} . This completes the dynamic analysis of link 3. The following are plots of the reaction force components of F_{43} (Figure 11.) and F_{53} (Figure 11.). The plot of F_{43} is shown instead of the calculated F_{34} because it relates to the first link we are analyzing, link 3, as opposed to link 4. As will be the case for all other iterations of this method, values after the "F", when switched, will be negatives of each other (i.e. $F_{43} = -F_{34}$).

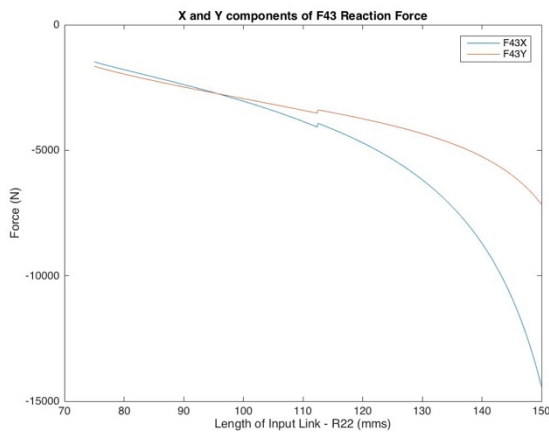


Figure 11 F_{43X} and F_{43Y}

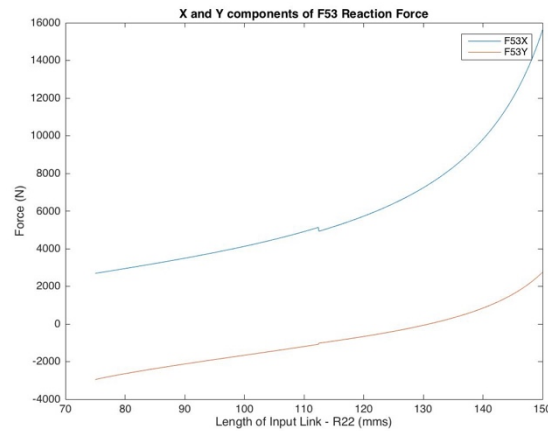


Figure 12a F_{53X} and F_{53Y}

The plotted trend lines of F_{43x} , F_{43y} , F_{53x} , and F_{53y} over the course of the move have a curve almost seemingly exponential because the angular acceleration of each link involved changes (α_4 and α_5 increase and α_3 decreases). F_{43} decreases while F_{53} increases. F_{43x} and F_{43y} in Figure.11 have similar values for the first portion of the move, but F_{43x} becomes significantly smaller for the second portion of the move. F_{53x} and F_{53y} have similar profiles in Figure.11a with F_{53x} increasing more dramatically for the second portion of the move, but the two values are offset by more than 4000 N. The tabulated data values of F_{43x} , F_{43y} , F_{53x} , and F_{53y} can be found in Appendix A.3.

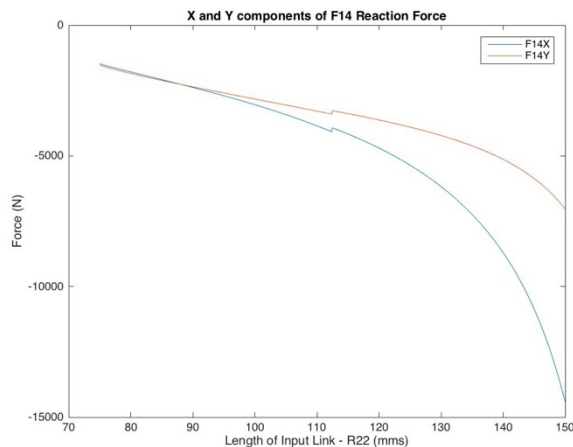


Figure 13 F_{14X} and F_{14Y}

In link 4, Eqns 8 and 9 can now be used to find F_{14x} and F_{14y} . These two values can be found because the acceleration of the center of mass of link 4 (G_4) is zero ($A_{G4x} = 0$ and $A_{G4y} = 0$ because it is pinned to the ground). The tabulated data for F_{14x} and F_{14y} can be found in Appendix A.5.

Because $F_{14x} = -F_{34x} = F_{43x}$, and $F_{14y} = F_{w4} - F_{34y} = F_{w4} + F_{43y}$ (this can be seen in Eqns 8 and 9), the plot of F_{14} in Figure.13 is nearly identical to that of F_{43} in Figure.11.

Similar to links 3 and 4, links 5 and 6 will be solved in conjunction. The original unknowns for link 5 are F_P , F_{65x} , and F_{65y} , and the unknowns on link 6 are F_{56x} , F_{56y} , F_{16x} , and F_{16y} . The free body diagrams (Link 5 = Figure.14, Link 6 = Figure.15) and symbolic equations for both links can be seen below.

$$\begin{aligned} \Sigma F_x &= F_{65x} + F_{35x} + F_P \cos(\theta_p) = m_5 A_{G5x} \text{ (Eqn. 11)} \\ \Sigma F_y &= F_{65y} + F_{35y} + F_P \sin(\theta_p) - F_{w5} = m_5 A_{G5y} \text{ (Eqn. 12)} \\ \Sigma M_P &= R_{5x} * F_{35y} - R_{5y} * F_{35x} + 2(R_{5x} * F_{65y} - R_{5y} * F_{65x}) - R_{5x} * F_{w5} = I_{G5} \alpha_5 + m_5 (R_{5x} * A_{G5y} - R_{5y} * A_{G5x}) \text{ (Eqn. 13)} \end{aligned}$$

$$\begin{aligned} \Sigma F_x &= F_{56x} + F_{16x} = m_6 A_{G6x} = 0 \text{ (Eqn. 14)} \\ \Sigma F_y &= F_{56y} + F_{16y} - F_{w6} = m_6 A_{G6y} = 0 \text{ (Eqn. 15)} \\ \Sigma M_{G6} &= R_{6x} * F_{56y} - R_{6y} * F_{56x} = I_{G6} \alpha_6 \text{ (Eqn. 16)} \end{aligned}$$

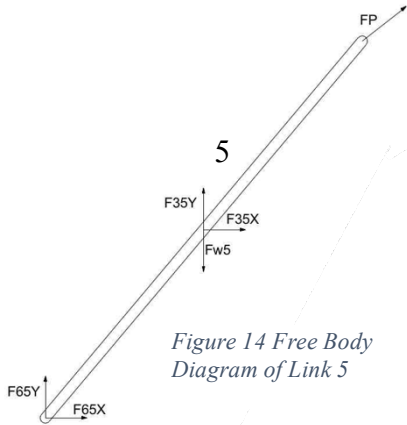


Figure 14 Free Body Diagram of Link 5

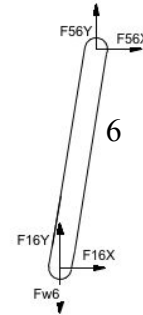


Figure 15 Free Body Diagram of Link 6

Similar to the process used for links 3 and 4, Eqns 13 and 16 can be reorganized to be in terms of F_{65} , and can be written in matrix formation. The resulting series of matrices are shown below:

$$\begin{bmatrix} -2R_{5y} & 2R_{5x} \\ R_{6y} & -R_{6x} \end{bmatrix} \begin{bmatrix} F_{65x} \\ F_{65y} \end{bmatrix} = \begin{bmatrix} I_{G5} \alpha_5 + m_5 * R_{5x} * A_{G5y} - m_5 * R_{5y} * A_{G5x} + R_{5x} * g * m_5 - R_{5x} * F_{35y} + R_{5y} * F_{35x} \\ I_{G6} \alpha_6 \end{bmatrix}$$

F_{65x} and F_{65y} can be solved at this point using Cramer's rule. Additionally, Eqn. 14 can then be used to solve for F_{16x} , and then Eqn. 15 can be used to solve for F_{16y} . These values can be found because the acceleration of G_6 is zero ($A_{G6x} = 0$, $A_{G6y} = 0$ because it is pinned to the ground). The tabulated values for F_{56x} , F_{56y} , F_{16x} , and F_{16y} can be found in Appendix A.5, and the plots of the components of F_{65} and F_{16} can be seen in Figure.16 and Figure.17 respectively.

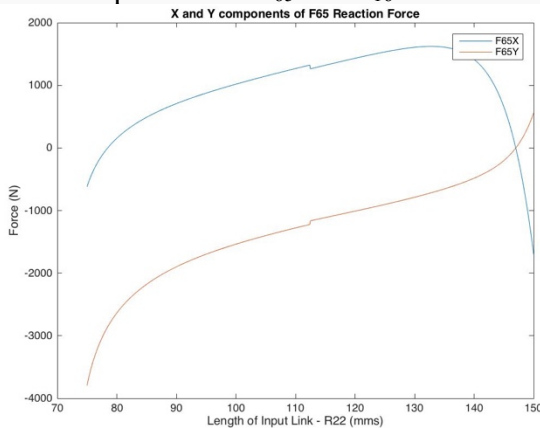


Figure 17 F_{65x} and F_{65y}

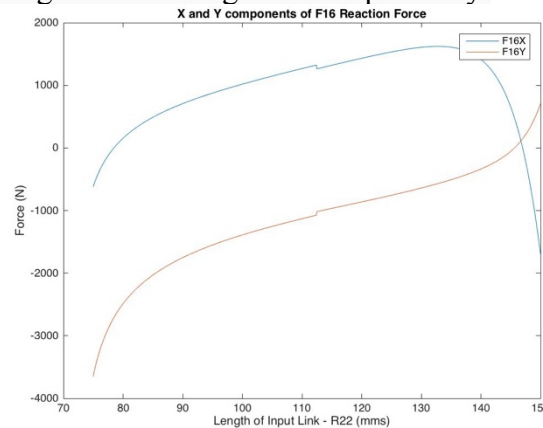


Figure 16 F_{16x} and F_{16y}

The plot of the components of F_{65} (Figure.16) and F_{16} (Figure.17) are nearly identical (as described in Eqns 14 and 15) which is to be expected. The X and Y components all have a large

slope originally which then evens out to a steady slope that continues for the majority of the move. After R_{22} increases past 135 mm, the slope of the X component increases while the slope of the Y component levels off and then falls until the end of the move.

F_P (on link 5) can be found through determining its components (X and Y) from Eqn. 11 and Eqn. 12 and then finding the magnitude of the vector from the components. The tangential component of F_P can be determined by multiplying the unit tangent of point P (calculated in earlier project) with F_P . The following equation describes this relationship:

$$F_{P,tangent} = \hat{U}_t \cdot F_P = \hat{U}_t x \cdot F_{Px} + \hat{U}_t y \cdot F_{Py}$$

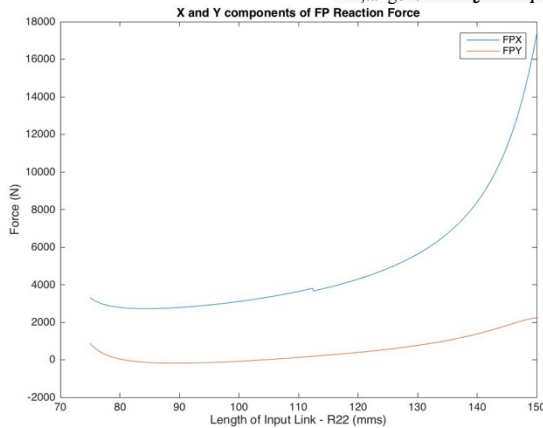


Figure 19 F_{PX} and F_{PY}

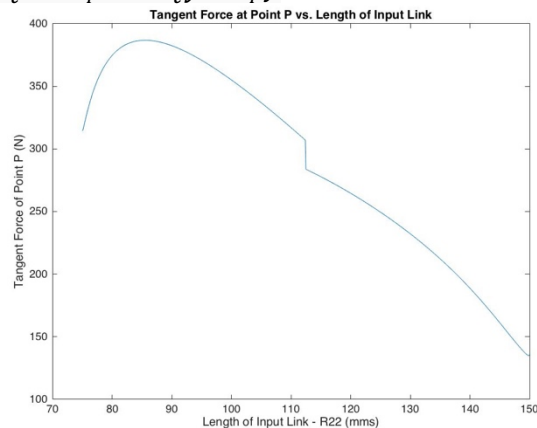


Figure 18a Tangent Component of F_{PX} and F_{PY}

The plot of the components of F_P in Figure.18 shows F_{PY} staying very small over the course of the move while F_{PX} gradually decreases until R_{22} is a little past 80 mm, and then increases in slope for the remainder of the move. The value of F_P at the end of the move is almost 9 times the value of F_P at the start. The tangential component of F_P along the path of point P shown in Figure.18a is almost parabolic as it increases in value for the first 15 mm, levels off, and then decreases in value for the remainder of the move. The only discrepancy in this plot description is at $R_{22} = 110$ mm, when R_{22} 's acceleration changes, and where there is a dramatic drop in value. It is consistently seen across all of the plots that there is a discrepancy in plot profiles at $R_{22} = 110$ mm, so this is not anything specifically remarkable. The tabulated data for the components of F_P and the tangential component of F_P can be found in Appendix A.5

Hydraulic Actuator to Purchase:



Product #1304K3

The hydraulic actuator that should be used for this application is from McMaster-Carr (Product #1304K3). It has a stroke of 3" and a maximum force of 5378 N. The actuator will cost \$155.51.

Depending on the particular design requirements, if the design team cannot afford to spend that much on a single actuator and the group doesn't mind that the actuator is used, I would suggest a used Cessna actuator (Product #9-10483) which also has a 3" stroke and a max force of 785 N, but it is priced at around \$39.95.



Product #9-10483

Dynamic force analysis through method of inspection when $R_{22} = 100$ mm has been completed on the following page:

II: Static Force Analysis of the Mechanism – Analytical Method

The free body diagrams for each link in static equilibrium are the same as the free body diagrams for dynamic analysis because the acceleration (or non-acceleration) of a link does not affect the fact that forces exist in particular locations on the link. Please refer to the following figures for the free body diagrams in this section.

Link 9 → Figure.2

Link 2 → Figure.6

Link 4 → Figure.9a

Link 6 → Figure.15

Link 8 → Figure.4

Link 3 → Figure.9

Link 5 → Figure.14

The symbolic equations for static analysis can be found below:

Link 9:

$$\Sigma F_x = F_{19x} + F_{29x} = m_9 A_{G9x} = 0 \text{ (Eqn. as)}$$

$$\Sigma F_y = F_{19y} + F_{29y} = m_9 A_{G9y} = 0 \text{ (Eqn. bs)}$$

$$\Sigma M_{O19} = R_{9x} * F_{29y} = I_{9} \alpha_9 = 0 \text{ (Eqn. cs)}$$

Link 8:

$$\Sigma F_x = F_{18x} + F_{28x} = m_8 A_{G8x} = 0 \text{ (Eqn. es)}$$

$$\Sigma F_y = F_{18y} + F_{28y} = m_8 A_{G8y} = 0 \text{ (Eqn. fs)}$$

$$\Sigma M_{O28} = R_{8x} * F_{28y} = I_{8} \alpha_8 = 0 \text{ (Eqn. gs)}$$

Link 2:

$$\Sigma F_x = F_{92x} + F_{32x} + F_{82x} + F_{12x} = m_2 A_{G2x} = 0 \text{ (Eqn. 1s)}$$

$$\Sigma F_y = F_{32y} + F_{12y} - F_{w2} = m_2 A_{G2y} = 0 \text{ (Eqn. 2s)}$$

$$\Sigma M_{G2} = T_2 + \rho * F_{12x} = I_{G2} \alpha_2 = 0 \text{ (Eqn. 3s)}$$

Link 3:

$$\Sigma F_x = F_{53x} + F_{43x} + F_{23x} = m_3 A_{G3x} \text{ (Eqn. 5s)}$$

$$\Sigma F_y = F_{53y} + F_{43y} + F_{23y} - F_{w3} = m_3 A_{G3y} \text{ (Eqn. 6s)}$$

$$\Sigma M_{O53} = R_{333x} * F_{43y} - R_{333y} * F_{43x} - R_{333x} * g * m_3 - (R_{333x} * F_{23y} - R_{333y} * F_{23x}) = I_{G3} \alpha_3 + m_3 * (R_{333x} * A_{G3y} - R_{333y} * A_{G3x}) = 0 \text{ (Eqn. 7s)}$$

Link 4:

$$\Sigma F_x = F_{14x} + F_{34x} = m_4 A_{G4x} = 0 \text{ (Eqn. 8s)}$$

$$\Sigma F_y = F_{14y} + F_{34y} - F_{w4} = m_4 A_{G4y} = 0 \text{ (Eqn. 9s)}$$

$$\Sigma M_{G4} = R_{4x} * F_{34y} - R_{4y} * F_{34x} = I_{G4} \alpha_4 = 0 \text{ (Eqn. 10s)}$$

Link 5:

$$\Sigma F_x = F_{65x} + F_{35x} + F_p \cos(\theta_p) = m_5 A_{G5x} = 0 \text{ (Eqn. 11s)}$$

$$\Sigma F_y = F_{65y} + F_{35y} + F_p \sin(\theta_p) - F_{w5} = m_5 A_{G5y} = 0 \text{ (Eqn. 12s)}$$

$$\Sigma M_P = R_{5x} * F_{35y} - R_{5y} * F_{35x} + 2(R_{5x} * F_{65y} - R_{5y} * F_{65x}) - R_{5x} * F_{w5} = I_{G5} \alpha_5 + m_5 (R_{5x} * A_{G5y} - R_{5y} * A_{G5x}) = 0 \text{ (Eqn. 13s)}$$

Link 6:

$$\Sigma F_x = F_{56x} + F_{16x} = m_6 A_{G6x} = 0 \text{ (Eqn. 14s)}$$

$$\Sigma F_y = F_{56y} + F_{16y} - F_{w6} = m_6 A_{G6y} = 0 \text{ (Eqn. 15s)}$$

$$\Sigma M_{G6} = R_{6x} * F_{56y} - R_{6y} * F_{56x} = I_{G6} \alpha_6 = 0 \text{ (Eqn. 16s)}$$

The static force analysis conducted using method of inspection when $R_{22} = 100$ mm can be seen on the next page:

The plots describing the static force analysis are quite similar to their dynamic force analysis counterparts, the only major change in profile is the absence of the abrupt shift at $R_{22} = 110$ mm. The plots of all reaction forces for static force analysis are shown below:

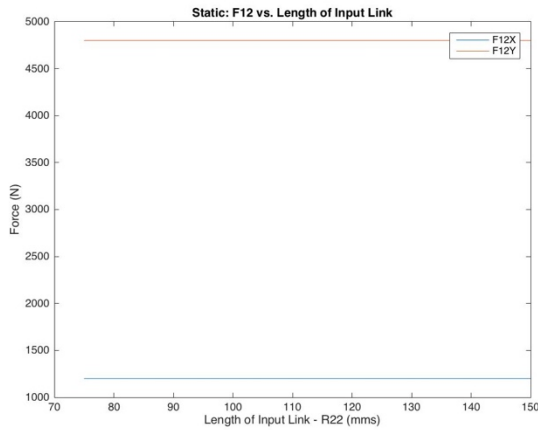


Figure 25a Static: F_{12X} and F_{12Y}

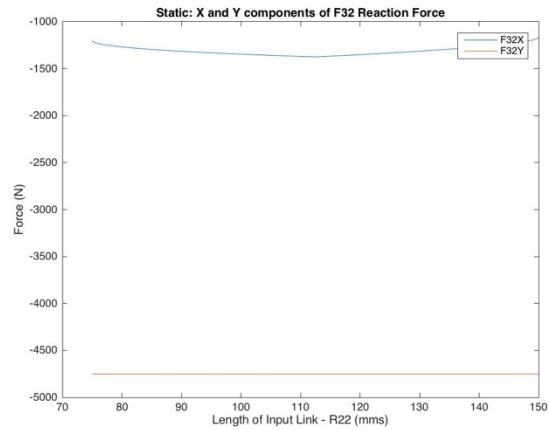


Figure 24a Static: F_{32X} and F_{32Y}

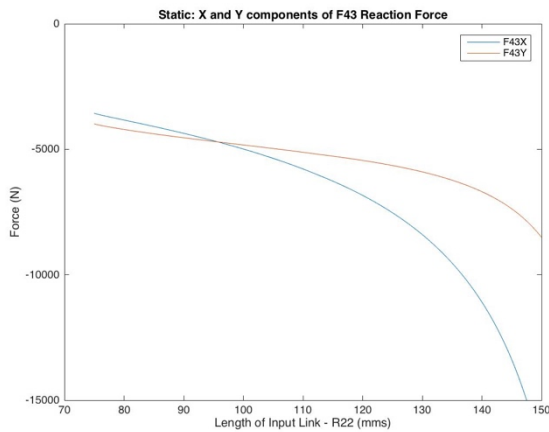


Figure 23b Static: F_{43X} and F_{43Y}

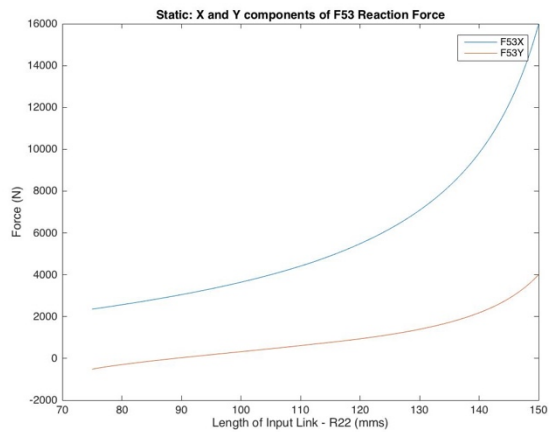


Figure 22c Static: F_{53X} and F_{53Y}

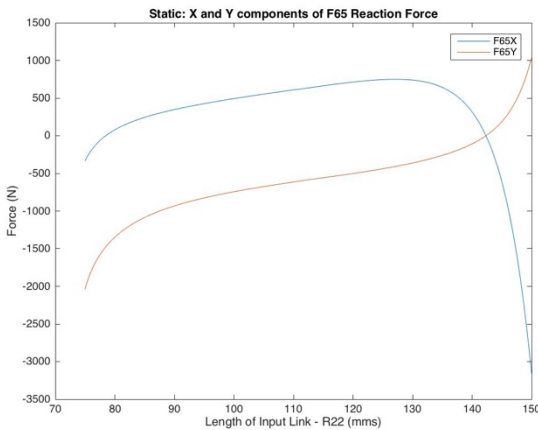


Figure 21 Static: F_{65X} and F_{65Y}

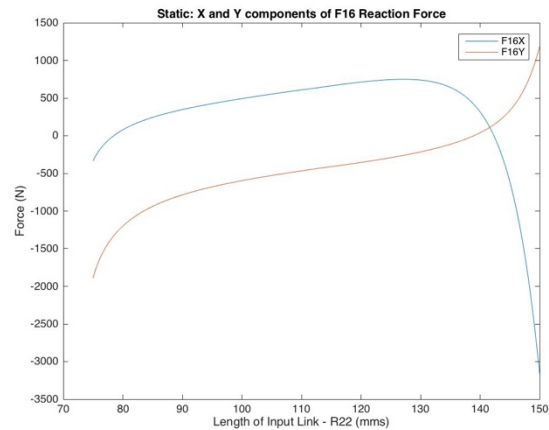


Figure 20 Static: F_{16X} and F_{16Y}

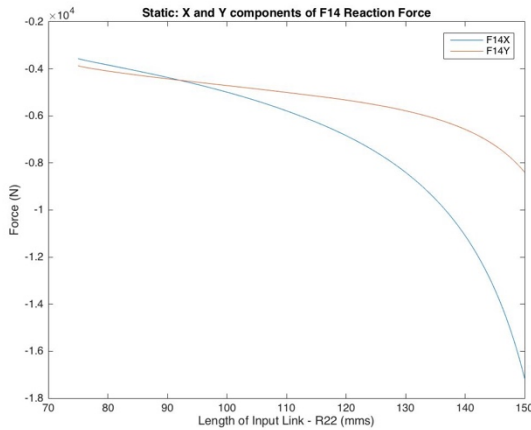


Figure 26a Static: F14X and F14Y

Tabulated values of the components of each reaction force during the move are located:

- F12 → Appendix B.2
- F23 → Appendix B.2
- F43 → Appendix B.3
- F53 → Appendix B.3
- F65 → Appendix B.4
- F16 → Appendix B.4
- F14 → Appendix B.5

II: Static Force Analysis of the Mechanism – Graphical Method

Type of Member

Link 2 is a 5-Force and a Torque member which can be simplified to a 2-Force and a Torque.

Link 3 is a 4-Force Member.

Link 4 is a 3-Force Member.

Link 5 is a 4-Force Member.

Link 6 is a 3-Force Member.

The graphical method will be conducted three separate times for $R_{22} = 100$ mm, the first iteration will neglect the force of gravity, the second will neglect the torque on link 2 (T_{12}), and the third will not exclude any external forces or torques. It is important to mention that all force polygons in this section will use a scale of 1" = 2000 N unless otherwise stated.

Iteration #1:

For the first iteration, the gravity in each link will be neglected.

Neglecting gravity, link 2 becomes a 4-Force and a Torque member.

F_{82} and F_{92} can be combined together to form a single force ($F_{82} + F_{92} = -12.5 + 158.11 = 145.61$ N $\angle 0.00^\circ$) and that force combined with the calculated F_{12} ($F_{12} = \sqrt{(F_{12x})^2 + (F_{12y})^2} = \sqrt{(-1200)^2 + (4800)^2} = 4947.7$ N $\angle 104.04^\circ$) reclassifies the link as a 2-Force and a Torque

member. The resultant force from the combination of $F_{82} + F_{92}$ and F_{12} can be seen in Figure.27b. Because the force polygon measures the length of F_{res1} as 2.457", F_{res1} is 4914 N $\angle 102.39^\circ$. F_{res1} and F_{32} are the only two forces present on the link, so they must be equal and opposite, so F_{32} must be 4914 N $\angle 282.39^\circ$. The final LOAs of each force on link 2 are shown in Figure.27a.

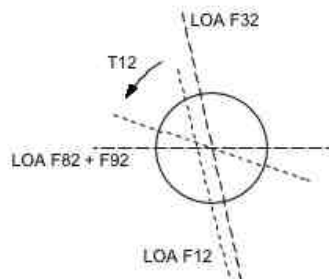


Figure 27a FBD of link 2 - Iteration #1

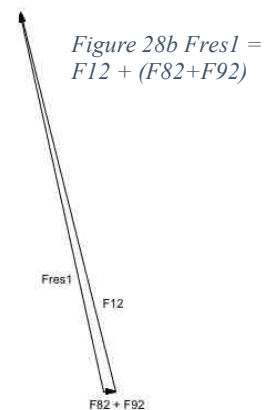


Figure 28b $F_{res1} = F_{12} + (F_{82} + F_{92})$

Link 4 is a 2-Force member when gravity is neglected (shown in Figure.29), so $F_{14} = -F_{34} = F_{43}$, and the LOA of both is directly through link 4. This assists us in completing our graphical analysis of link 3.

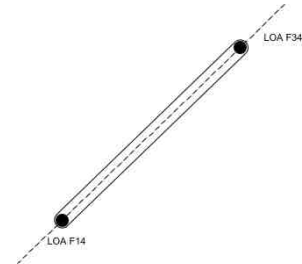


Figure 29 FBD of link 4 - Iteration #1

When gravity is neglected, link 3 is a 3-Force member, and the direction of F_{43} and magnitude and direction of F_{23} are known, so the direction of F_{53} is also known because all three LOAs must meet at one particular point. The LOAs can be seen in Figure.30. Using the force polygon shown in Figure.31, the values of F_{43} and F_{53} can be found. $F_{43} = 4436 \text{ N} \angle 224.05^\circ$, and $F_{53} = 4577 \text{ N} \angle 337.98^\circ$. As stated above, $F_{14} = F_{43}$, so $F_{14} = 4436 \text{ N} \angle 224.05^\circ$. The LOAs for F_{14}

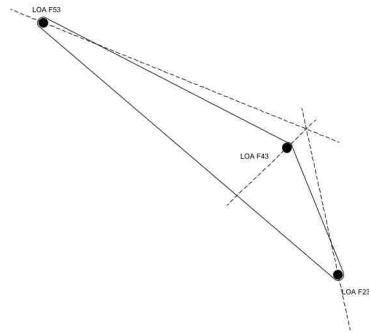


Figure 31 FBD of link 3 - Iteration #1

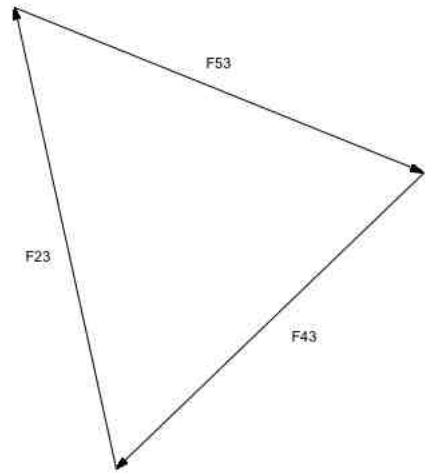


Figure 30 $F_{23} + F_{43} + F_{53} = 0$

and F_{34} on link 4 can be seen in Figure.29.

Similar to link 4, link 6 is a two force member when gravity is neglected, and therefore $F_{56} = F_{16}$ and the LOA of both forces is directly through the link (this is shown in Figure.30a). This knowledge will allow us to solve for the forces on link 5.

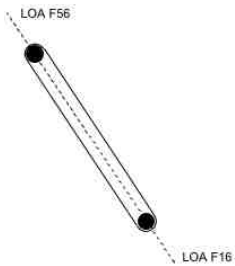


Figure 32a FBD of link 6 - Iteration #1

On link 5, we know the magnitude and direction of F_{35} , and the direction of F_{65} (same LOA as F_{56}). Because without gravity link 5 is a 3 force member, the direction of F_P can be found because all LOAs must meet at a single point. The free body diagram of link 5 is found below as Figure.33 in addition to the force polygon(Figure.34) used to solve for F_{65} and F_P . From the force polygon, F_{65} is $1916 \text{ N} \angle 303.53^\circ$ and F_P is $3187 \text{ N} \angle 357.86^\circ$. Returning to Figure.30a, where $F_{16} = -F_{56} = F_{65}$, F_{16} is now known as $1916 \text{ N} \angle 303.53^\circ$.

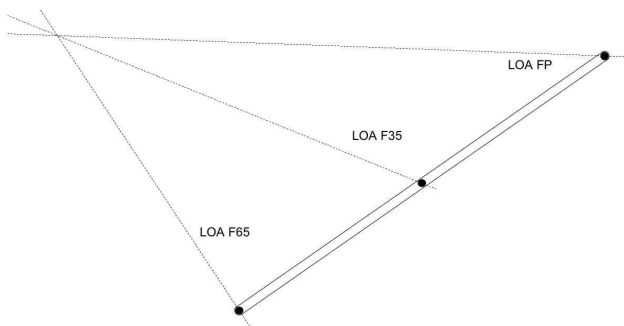


Figure 34 FBD of link 5 - Iteration #1

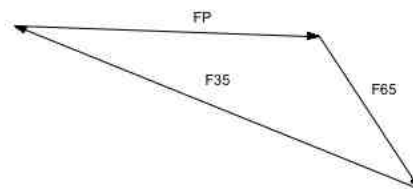


Figure 33 $F_p + F_{65} + F_{35} = 0$

Iteration #2

For the second iteration, the torque in link 2 will be neglected.

Neglecting T12, link 2 becomes a 4-Force member because F12 is solely determined by T12, and if T12 is neglected F12 is nonexistent also. Fw2, F82, and F92 can be combined together to form a single force ($Fw2+F82+F92 = -12.5i+158.1139j = 145.6139i-49.05j = 153.6532 \text{ N} \angle 341.38^\circ$) and with F32 the link can be reclassified as a 2-Force member. Thus F32 must be equal and opposite to the combination force of Fw2, F82, and F92 and have a magnitude and direction of $153.6532 \text{ N} \angle 161.38^\circ$. The free body diagram with the final force LOAs are shown in Figure.35.

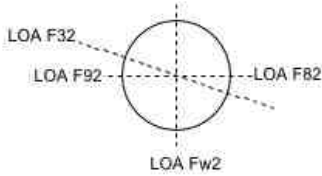


Figure 35 FBD of link 2 - Iteration #2

Link 3 is a 4-Force member when T12 is neglected, so the two known forces (Fw3 and F23) will be combined to create a resultant force (Fres2). The force polygon for this is shown in Figure.36. From Figure.36, $Fres2 = 244 \text{ N} \angle 233.42^\circ$. From determining the magnitude and direction of Fres2, we can now determine the magnitude and direction of F43 and F53 using the force polygon shown in Figure.36a. F43 is $316 \text{ N} \angle 44.05^\circ$ and F53 is $85 \text{ N} \angle 196.13^\circ$. The final LOAs for each force on link 3 are shown in Figure.36b.



Figure 36 $Fres2 = Fw3 + F23$



Figure 38a $Fres2 + F43 + F53 = 0$

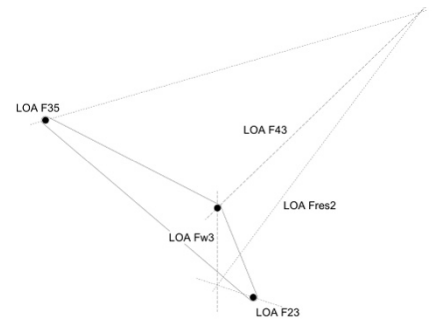


Figure 37b FBD of link 3 - Iteration #2

Figure 40a FBD of link 4 - Iteration #2

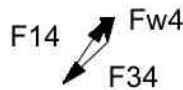
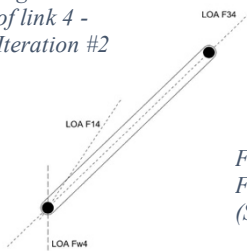


Figure 39
 $F14+Fw4+F34=0$
(SCALE: 1"=1000N)

Link 4 is a 3-Force member, and the magnitude and direction of F14 can be determined from a force polygon with Fw4 and F34. Figure.39 shows the required force polygon, and from this force polygon F14 is $407 \text{ N} \angle 56.05^\circ$. The final LOAs on link 4 are shown in Figure.39a.

Similar to link 4, link 6 is a 3-Force member when T12 is neglected, where the LOA of F56 will be through link 6. This will assist in solving for forces on link 5.

On link 5, we know the magnitude and direction of F35, the magnitude and direction of Fw5, and the direction of F65 (same LOA as F56). A resultant force (Fres3) is found by combining F35 and Fw5 (Force polygon shown in Figure.41), and using this resultant force, the magnitude of F56 and the magnitude and direction of FP can be found by the force polygon shown to the

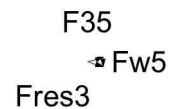


Figure 41 $F35 + Fw5 = Fres3$



Figure 43 $Fres3 + FP + F65 = 0$
(SCALE: 1"=1000N)

left in Figure.42. From the force polygon shown in Figure.42, F65 is $34 \text{ N} \angle 123.53^\circ$ and FP is $63 \text{ N} \angle 182.18^\circ$. The final force LOAs on link 5 are shown to the left in Figure.41a.

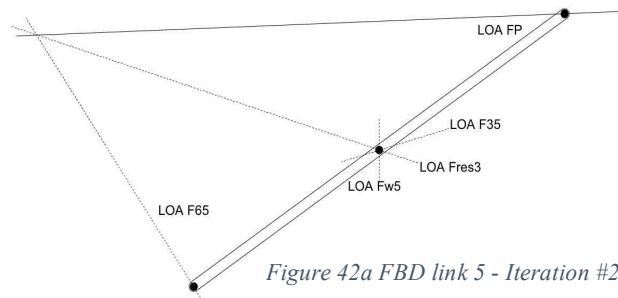


Figure 42a FBD link 5 - Iteration #2

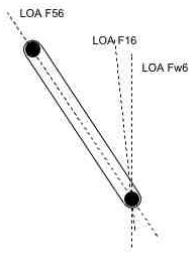


Figure 45 FBD of link 6 - Iteration #2

Returning to link 6 and Figure.44, a force polygon can be created to solve for the magnitude and direction of F16. From this force polygon, F16 is 176 N \angle 96.10°. This force polygon is shown in Figure.45, and the final force LOAs on link are shown in Figure.44.

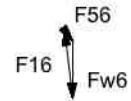


Figure 44 $F16 + F56 + Fw6 = 0$
(SCALE: 1"=1000N)

Iteration #3:

For the third iteration, nothing will be neglected. Link 2 is a 5-Force member with Torque. Fw2, F82, and F92 can be combined together to form a single force ($Fw2+F82+F92 = -12.5i+158.1139i = 145.6139i-49.05j = 153.6532 \text{ N} \angle 341.38^\circ$) and F12 can be found by taking the moment about G2 to find F12X and then finding F12Y using the frictional coefficient. This process is shown below:

$$\Sigma M_{G2} = 12.5F12X + -T12*1000 = IG2*\alpha_2 \rightarrow F12X = (IG2*\alpha_2 - T12*1000)/(12.5) = -1200 \text{ N}$$

$$F12Y = \text{abs}(F12X/\mu) = 4800 \text{ N}$$

The direction of F12 is determined by the equation:

$$\Phi = \tan^{-1}(\mu) = \tan^{-1}(0.25) = 14.036^\circ$$

Thus F12 can be found by taking the magnitude of the component values and taking Φ from the vertical axis.

$$F12 = \text{sqrt}((F12x)^2 + (F12y)^2) = \text{sqrt}((-1200)^2 + (4800)^2)$$

$$F12 = 4947.7 \text{ N} \angle 104.04^\circ$$

A force polygon can then be used to determine the magnitude and direction of Fres4. Because the link has been reduced down to 2-Forces and a Torque (Fres4, F32, and T12), F32 has to be equal but opposite to Fres4. Because the force polygon shown in Figure.46 determines Fres4 to be 4867 N \angle 102.51°, F32 must be 4867 N \angle 282.51°. The final LOAs of all forces on link 2 are shown in Figure.47.

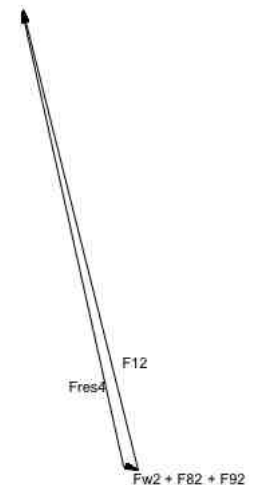


Figure 46 $Fres4 = Fw2 + F82 + F92 + F12$

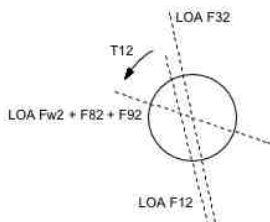


Figure 47 FBD of link 2 - Iteration #3

Link 3 will be solved by creating a resultant force (Fres5) of Fw3 and F23 (Figure.48), and then using a force polygon with F53, F43 and Fres5 (Figure.50) to determine the magnitude and direction of both F53 and F43. The two necessary force polygons (Figure.48 and Figure.50) and the free body diagram (Figure.49) with all relevant LOAs are shown on the next page.



Figure 50 $F_{w3} + F_{23} = F_{res5}$

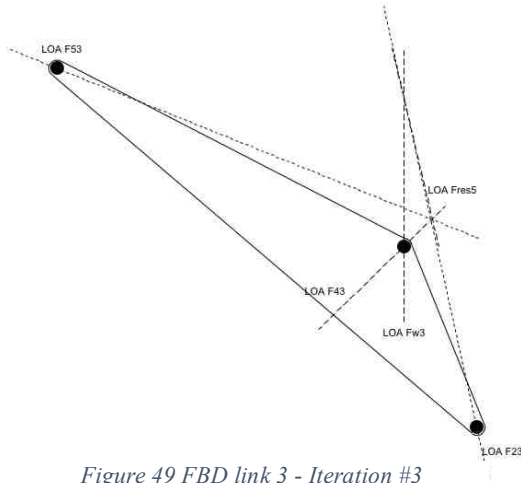


Figure 49 FBD link 3 - Iteration #3

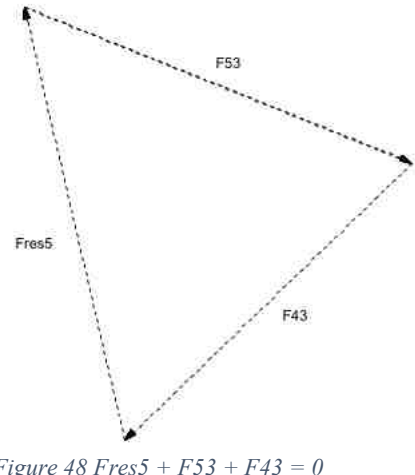


Figure 48 $F_{res5} + F_{53} + F_{43} = 0$

Using this method, F_{43} is determined to be $4157\text{ N} \angle 225^\circ$ and F_{53} is $4356\text{ N} \angle 338.13^\circ$.

A force polygon will also be used to solve link 4. The force polygon used (Figure.51a) and the LOAs of each relevant force (Figure.51) are shown below. F_{14} is determined to be $4076\text{ N} \angle 222.86^\circ$.

Figure 52 FBD link 4 - Iteration #3

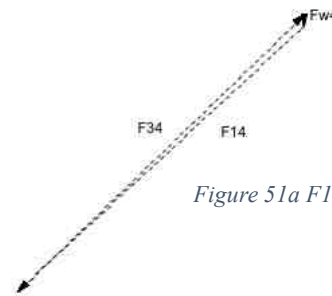
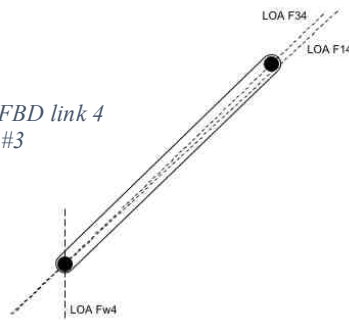
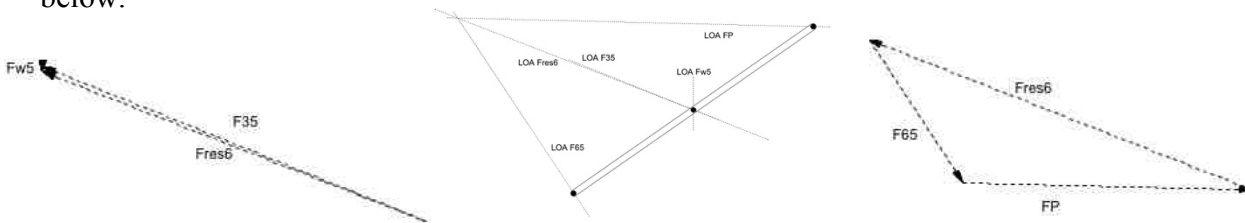


Figure 51a $F_{14} + F_{34} + F_{w4} = 0$

Similar to link 4, link 6 will have two forces (F_{16} and F_{w6}) through one pin joint of the link, so the third force (F_{56}) must go through the link. Thus we know the direction of F_{56} .

In link 5, the magnitude and direction of F_{35} and F_{w5} are known, and because we know the direction of F_{65} , we can find the resultant force of F_{35} and F_{w5} , and then use a force polygon to find the magnitude and direction of F_P , and the magnitude of F_{65} . The force polygon showing the creation of the resultant force of F_{35} and F_{w5} (F_{res6}), the force polygon which allows for the determining of F_{65} and F_P , and the final LOAs of all forces on link 5 can be seen below.



From Figure X, F_{65} is $1800\text{ N} \angle 303.53^\circ$ and F_P is $3049\text{ N} \angle 358.62^\circ$.

Link 6 will be solved very similarly to link 4, and the force polygon used (Figure.53) and the LOAs of each relevant force (Figure.54) are shown below. F16 is determined to be 1679 N \angle 306.30°.

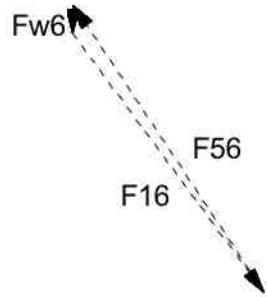


Figure 53 $F_{w6} + F_{16} + F_{56} = 0$

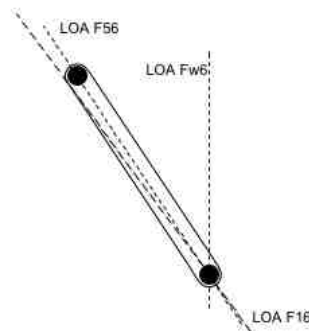


Figure 54 FBD link 6 - Iteration #3

Iteration Comparison

From interpreting the values for each internal reaction force in each iteration, it is evident that there is a pattern. The sum of the Iteration 1 and Iteration 2 values of every force (in its x and y components) is very close to the Iteration 3 force. See below in Table.1 for calculations to prove this idea.

Table 1: Iteration Force Component Comparison

Iteration	F32		F43		F53		F14		F65		FP		F16	
	X	Y	X	Y	X	Y	X	Y	X	Y	X	Y	X	Y
#1	1054	-4800	-3188	-3084	4243	-1716	-3188	-3084	1058	-1597	3185	-119	1058	-1597
#2	-145	49	227	220	-82	-24	227	338	-19	28	-63	-2	-19	175
#1 + #2	909	-4751	-2961	-2864	4161	-1740	-2961	-2746	1039	-1569	3122	-121	1039	-1422
#3	1054	-4751	-2939	-2939	4043	-1623	-2988	-2773	994	-1500	3048	-73	994	-1353

The slight variation between the values in the last two rows is due to rounding of Iteration #1/#2 force values in order to fit numbers in the table cells. It is important to see the overall pattern, and how the numbers are close. It can be concluded from the above tables that the summation of all iterations with an element neglected in theory will hold the same amount of force as the iteration with no elements neglected.

Analytical and Graphical Comparison

The internal reaction forces for this mechanism (in their x and y components) for both the Analytical and Graphical solution methods are shown below in Table.2.

Table 2 Force Component Comparison between Analytical and Graphical Solution Method

	F32		F43		F53		F14		F65		FP		F16	
Iteration	X	Y	X	Y	X	Y	X	Y	X	Y	X	Y	X	Y
Analytical	1054	-4751	-2983	-2885	4037	-1620	-2983	-2768	995	-1501	3042	-77	995	-1354
Graphical	1054	-4751	-2939	-2939	4043	-1623	-2988	-2773	994	-1500	3048	-73	994	-1353

The values for the components of each internal reaction force are almost exactly the same between the Analytical and the Graphical solution method. Some components have larger differences than others, and these differences are largely due to rounding during calculation. This is a good check to ensure that the analytical method was determined correctly. As long as a particular set of rules are followed, the graphical method will always be correct, so the fact that the values for the analytical and graphical methods are almost exact proves that the analytical method was completed correctly.

III: The Equation of Motion

The power equation for this mechanism will begin with the basic form of:

$$P = \Delta T + \Delta U + \Delta W_f$$

where P = Net Power, T = Kinetic Energy, U = Potential Energy, and W_f = Work due to external forces.

Each term must now be defined for this particular mechanism, and they will each be defined symbolically as well as for a particular instant ($R_{22} = 100\text{mm}$) during the move. The process to determine the terms is shown below.

Equivalent Mass Moment of Inertia

First the mass moments of inertia of each link in the mechanism must be calculated. The basic form for mass moment of inertia is $A_x = m_x((x_{GX}')^2 + (y_{GX}')^2) + I_{GX}(\theta_x'^2)$, and thus the mass moment of inertia for each link is written below.

$$A_2 = m_2(1) + I_{G2}(\theta_2')^2 = m_2 + I_{G2}(\theta_2')^2$$

$$A_3 = m_3((x_{G3}')^2 + (y_{G3}')^2) + I_{G3}(\theta_3')^2$$

$$A_4 = m_4(0) + I_{G4}(\theta_4')^2 = I_{G4}(\theta_4')^2$$

$$A_5 = m_5((x_{G5}')^2 + (y_{G5}')^2) + I_{G5}(\theta_5')^2$$

$$A_6 = m_6(0) + I_{G6}(\theta_6')^2 = I_{G6}(\theta_6')^2$$

Because the center of mass does not move in links 4 and 6, the first portion of their equations are "0". Similarly, R_2 is moving with the input, so its center of mass's change in position is "1".

The equivalent mass moment of inertia is the sum of all of these values ($\Sigma A = A_2 + A_3 + A_4 + A_5 + A_6$), and it will be used to calculate the change in kinetic energy in the system.

$\Sigma A =$ Equivalent Mass Moment of Inertia

$$= A_2 + A_3 + A_4 + A_5 + A_6 = m_2 + I_{G2}(\theta_2')^2 + m_3((x_{G3}')^2 + (y_{G3}')^2) + I_{G3}(\theta_3')^2 + I_{G4}(\theta_4')^2 + m_5((x_{G5}')^2 + (y_{G5}')^2) + I_{G5}(\theta_5')^2 + I_{G6}(\theta_6')^2$$

$$\begin{aligned} \text{When } R_{22} = 100 \text{ mm} \rightarrow \Sigma A &= 5 + 30(-0.08^2) * 1000 + 25((0.2812)^2 + (-0.2907)^2) \\ &+ 450(0.0103^2) * 1000 + 75(-0.004^2) * 1000 + 5((-0.4269)^2 \\ &+ (-1.6703)^2) + 250(-0.0077^2) * 1000 + 20(0.0209^2) * 1000 \\ &= 288.8851 \text{ kg} \end{aligned}$$

Thus the equivalent mass moment of inertia when $R_{22} = 100 \text{ mm}$ is 288.8851 kg. The equivalent mass moment of inertia in 2.5 mm increments is stated in Appendix.C1.

Another important calculation is necessary for each link, and it has the basic formula

$B_x = m_x(x_{GX}' * x_{GX}'' + y_{GX}' * y_{GX}'') + I_{GX}(\theta_x' * \theta_x'')$. Each link's version of this equation and the sum of all of the links equations are shown below.

$$B_2 = I_{G2}(\theta_2' * \theta_2'')$$

$$B_3 = m_3(x_{G3}' * x_{G3}'' + y_{G3}' * y_{G3}'') + I_{G3}(\theta_3' * \theta_3'')$$

$$B_4 = I_{G4}(\theta_4' * \theta_4'')$$

$$B_5 = m_5(x_{G5}' * x_{G5}'' + y_{G5}' * y_{G5}'') + I_{G5}(\theta_5' * \theta_5'')$$

$$B_6 = I_{G6}(\theta_6' * \theta_6'')$$

$$\begin{aligned} \Sigma B &= B_2 + B_3 + B_4 + B_5 + B_6 \\ &= I_{G2}(\theta_2' * \theta_2'') + m_3(x_{G3}' * x_{G3}'' + y_{G3}' * y_{G3}'') + I_{G3}(\theta_3' * \theta_3'') + I_{G4}(\theta_4' * \theta_4'') \\ &+ m_5(x_{G5}' * x_{G5}'' + y_{G5}' * y_{G5}'') + I_{G5}(\theta_5' * \theta_5'') + I_{G6}(\theta_6' * \theta_6'') \end{aligned}$$

$$\begin{aligned} \text{When } R_{22} = 100 \text{ mm} \rightarrow \Sigma B &= 30(-0.08 * 0) * 1000^2 + 25(0.2812 * 0.0044 \\ &- 0.2907 * -0.0069) * 1000 + 450(0.0103 * -0.00002) * 1000^2 \\ &+ 75(-0.004 * -0.00008) * 1000^2 + 5(-0.4269 * 0.02 \\ &+ (-1.6703) * (-0.0116)) * 1000 + 250(-0.0077 * -0.000046) * 1000^2 \\ &+ 20(0.0209 * -0.00031) * 1000^2 \\ &= -150.5385 \end{aligned}$$

The center of masses of Links 2, 4 and 6 do not accelerate during the move, so portions of those link's equations have been emitted.

Change in Kinetic Energy

After both sums have been calculated, the change in kinetic energy (ΔT) can be found. The kinetic energy represents the amount of energy present from motion, and the basic form for calculating it is shown below.

$$\Delta T = \frac{1}{2} \Sigma A * \dot{\psi} + \Sigma B * (\dot{\psi})^2$$

This can be rewritten for this mechanism's purposes as: $\Delta T = \frac{1}{2} \Sigma A * \ddot{R}_{22} + \Sigma B * (\dot{R}_{22})^2$

Substituting in the calculated values for ΣA and ΣB , ΔT is as follows.

$$\Delta T = \frac{1}{2}(m_2 + I_{G2}(\theta_2')^2) + m_3((x_{G3}')^2 + (y_{G3}')^2) + I_{G3}(\theta_3')^2 + I_{G4}(\theta_4')^2 + m_5((x_{G5}')^2 + (y_{G5}')^2) + I_{G5}(\theta_5')^2 + I_{G6}(\theta_6')^2) * \ddot{R}_{22} + (I_{G2}(\theta_2' * \theta_2'') + m_3(x_{G3}' * x_{G3}'' + y_{G3}' * y_{G3}'') + I_{G3}(\theta_3' * \theta_3'') + I_{G4}(\theta_4' * \theta_4'') + m_5(x_{G5}' * x_{G5}'' + y_{G5}' * y_{G5}'') + I_{G5}(\theta_5' * \theta_5'') + I_{G6}(\theta_6' * \theta_6'')) * (\dot{R}_{22})^2$$

$$\text{When } R_{22} = 100 \text{ mm} \rightarrow \Delta T = \frac{1}{2} (288.88)*0.125 + (-150.5385)* (79.05/1000)^2 = 35.1698 \text{ W}$$

Change in Potential Energy

Next, the change in potential energy (ΔU) will be found. Potential energy is the energy a body has due to its position in association with other bodies. In this mechanism there are two forms of potential energy, gravitational potential energy (U_G) and spring potential energy (U_S). The total change in potential will be the sum of the gravitational and spring potential energies as seen by the basic formula below.

$$\Delta U = \Delta U_G + \Delta U_S$$

U_G will deal solely with links 3 and 5, because the centers of mass on links 2, 4, and 6 do not change position over the course of the move. The change in gravitational potential energy is generally defined as the weight of the link multiplied by the change in height of the center of mass which can be rewritten for this mechanism as:

$$\Delta U_G = (m_3 * g)y_{G3}' + (m_5 * g)y_{G5}'$$

$$\text{When } R_{22} = 100 \text{ mm} \rightarrow \Delta U_G = (25*9.81)*-0.2907 + (5*9.81)*-1.6703 = -153.234 \text{ W}$$

U_S will deal with link 8 (the spring), and spring potential energy is determined by the spring coefficient multiplied by the change in length from the resting spring length. For this mechanism the spring potential energy can be written as:

$$\Delta U_S = k((R_{11} - R_{22}) - R_S) * R_S'$$

$$\text{When } R_{22} = 100 \text{ mm} \rightarrow \Delta U_S = 500((185-100)-110)/1000*1 = -12.5 \text{ W}$$

$$\text{Thus } \Delta U = \Delta U_G + \Delta U_S = (m_3 * g)y_{G3}' + (m_5 * g)y_{G5}' + k * (R_S + (R_{22} - R_{11}))$$

$$\text{When } R_{22} = 100 \text{ mm} \rightarrow \Delta U = -153.234 - 12.5 = -165.734 \text{ W}$$

Work due to External Forces

Because of the particular mechanism, the only work is due to friction, and so $\Delta W_f = F_{12}x$.

$$\text{Thus, when } R_{22} = 100 \text{ mm} \rightarrow \Delta W_f = F_{12}x = -1200 \text{ W}$$

Power Equation

All portions of the equation of motion are known now, so we can rewrite the power equation specifically for this mechanism.

$$P = \Delta T + \Delta U + \Delta W_f$$

$$P = \frac{1}{2}(m_2 + I_{G2}(\theta_2')^2) + m_3((x_{G3}')^2 + (y_{G3}')^2) + I_{G3}(\theta_3')^2 + I_{G4}(\theta_4')^2 + m_5((x_{G5}')^2 + (y_{G5}')^2) + I_{G5}(\theta_5')^2 + I_{G6}(\theta_6')^2) * \ddot{R}_{22} + (I_{G2}(\theta_2' * \theta_2'') + m_3(x_{G3}' * x_{G3}'' + y_{G3}' * y_{G3}'') + I_{G3}(\theta_3' * \theta_3'') + I_{G4}(\theta_4' * \theta_4'') + m_5(x_{G5}' * x_{G5}'' + y_{G5}' * y_{G5}'') + I_{G5}(\theta_5' * \theta_5'') + I_{G6}(\theta_6' * \theta_6'')) * (\dot{R}_{22})^2 + (m_3 * g)y_{G3}' + (m_5 * g)y_{G5}' + k * (R_S + (R_{22} - R_{11})) + F_{12}x_S$$

$$\text{When } R_{22} = 100 \text{ mm} \rightarrow P = 35.1698 - 140.734 - 1200 = -1330.6 \text{ W}$$

Percent Contribution

The percent contribution of each variable in the power equation can be determined by the following equations:

$$T\% = \frac{abs(\Delta T)}{abs(\Delta T)+abs(\Delta U_G)+abs(\Delta U_S)+abs(\Delta W_f)} = \frac{35.1698}{35.1698+153.234+12.5+1200} = 0.0251 \rightarrow 2.51\%$$

$$U\% = \frac{abs(\Delta U)}{abs(\Delta T)+abs(\Delta U_G)+abs(\Delta U_S)+abs(\Delta W_f)} = \frac{153.234+12.5}{35.1698+153.234+12.5+1200} = 0.1183 \rightarrow 11.83\%$$

$$W\% = \frac{abs(\Delta W_f)}{abs(\Delta T)+abs(\Delta U_G)+abs(\Delta U_S)+abs(\Delta W_f)} = \frac{1200}{35.1698+153.234+12.5+1200} = 0.8566 \rightarrow 85.66\%$$

This shows that friction holds the greatest amount of the contribution to power. Potential energy contributes the next largest amount of power, and the kinetic energy provides the least amount of power to the system.

Tangential Component of F_P

The tangential component of F_P can be determined by reordering the power equation to read:

$$F_P \tan = \frac{T_{12} * \theta'_2 - P}{R_P'}$$

The plot of $F_P \tan$ is shown below in Figure.55.

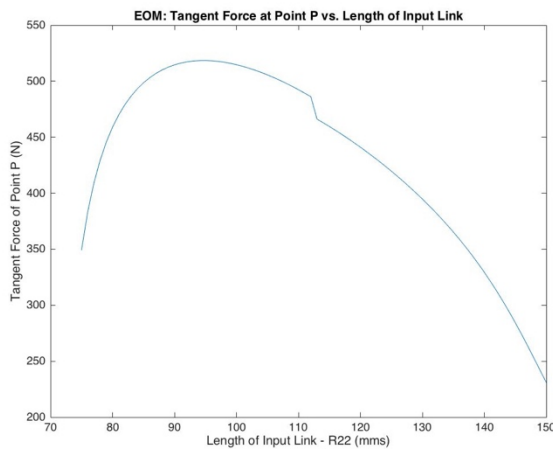


Figure 55 EOM: Tangent Component of FPX and FPY

The plot of the tangent component of F_P using the equation of motion (See Figure.55) is more rounded than the tangent component of F_P from dynamic analysis (See Figure.18a) because it refers to the transfer of energy for its values and not \ddot{R}_{22} , which flips at $R = 110$ mm.

IV: Conclusion

This assignment took its toll as it was similar analysis completed many different ways, and that became rather confusing when it became necessary to return and check on each method. In addition, the fact that each calculated value relied on many others required that each individual step be correct because one miscalculated instant or a displaced negative sign could transform the analysis and make all of the following calculated values incorrect. It was evident how the different ways of analysis affected the calculated values, and it was interesting to look at the different force profiles and try to distinguish why certain methods calculated force values closer or farther to the actual values. All in all, this assignment was difficult but quite rewarding because of how much it was able to teach about the analysis of a system.

V: Appendix

Appendix A.1 – External Forces, Dynamic

R22: (mm)	Actuator Force: (N)	Spring Force: (N)
75.0	0.00	0.00
77.5	50.00	-1.25
80.0	70.71	-2.50
82.5	86.60	-3.75
85.0	100.00	-5.00
87.5	111.80	-6.25
90.0	122.47	-7.50
92.5	132.29	-8.75
95.0	141.42	-10.00
97.5	150.00	-11.25
100.0	158.11	-12.50
102.5	165.83	-13.75
105.0	173.21	-15.00
107.5	180.28	-16.25
110.0	187.08	-17.50
112.5	193.65	-18.75
115.0	187.08	-20.00
117.5	180.28	-21.25
120.0	173.21	-22.50
122.5	165.83	-23.75
125.0	158.11	-25.00
127.5	150.00	-26.25
130.0	141.42	-27.50
132.5	132.29	-28.75
135.0	122.47	-30.00
137.5	111.80	-31.25
140.0	100.00	-32.50
142.5	86.60	-33.75
145.0	70.71	-35.00
147.5	50.00	-36.25
150.0	0.00	-37.50

Appendix A.2 – Link 2, Dynamic

R22: (mm)	F12X: (N)	F12Y: (N)	F23X: (N)	F23Y: (N)
75.0	-1224	4896	-1224.62	4846.95
77.5	-1224	4896	-1175.88	4846.95
80.0	-1224	4896	-1156.41	4846.95
82.5	-1224	4896	-1141.77	4846.95
85.0	-1224	4896	-1129.62	4846.95
87.5	-1224	4896	-1119.07	4846.95
90.0	-1224	4896	-1109.65	4846.95
92.5	-1224	4896	-1101.09	4846.95
95.0	-1224	4896	-1093.20	4846.95
97.5	-1224	4896	-1085.88	4846.95
100.0	-1224	4896	-1079.01	4846.95
102.5	-1224	4896	-1072.54	4846.95
105.0	-1224	4896	-1066.42	4846.95
107.5	-1224	4896	-1060.60	4846.95
110.0	-1224	4896	-1055.04	4846.95
112.5	-1176	4704	-1000.48	4654.95
115.0	-1176	4704	-1008.29	4654.95
117.5	-1176	4704	-1016.35	4654.95
120.0	-1176	4704	-1024.67	4654.95
122.5	-1176	4704	-1033.29	4654.95
125.0	-1176	4704	-1042.26	4654.95
127.5	-1176	4704	-1051.62	4654.95
130.0	-1176	4704	-1061.45	4654.95
132.5	-1176	4704	-1071.84	4654.95
135.0	-1176	4704	-1082.90	4654.95
137.5	-1176	4704	-1094.82	4654.95
140.0	-1176	4704	-1107.88	4654.95
142.5	-1176	4704	-1122.52	4654.95
145.0	-1176	4704	-1139.66	4654.95
147.5	-1176	4704	-1161.62	4654.95
150.0	-1176	4704	-1212.88	4654.95

Appendix A.3 – Link 3,
Dynamic

R22: (mm)	F43X: (N)	F43Y: (N)	F53X: (N)	F53Y: (N)
75.0	-1466.71	-1639.64	2691.68	-2962.37
77.5	-1638.97	-1816.83	2815.42	-2785.39
80.0	-1788.24	-1962.52	2945.42	-2639.89
82.5	-1934.87	-2099.14	3077.56	-2503.45
85.0	-2081.68	-2229.50	3212.36	-2373.26
87.5	-2230.31	-2355.07	3350.57	-2247.84
90.0	-2382.07	-2476.91	3493.00	-2126.16
92.5	-2538.09	-2595.85	3640.54	-2007.37
95.0	-2699.49	-2712.64	3794.13	-1890.72
97.5	-2867.39	-2827.98	3954.77	-1775.54
100.0	-3042.98	-2942.52	4123.55	-1661.16
102.5	-3227.56	-3056.93	4301.71	-1546.92
105.0	-3422.55	-3171.87	4490.62	-1432.15
107.5	-3629.58	-3288.08	4691.86	-1316.13
110.0	-3850.48	-3406.30	4907.24	-1198.10
112.5	-3927.06	-3390.19	4927.24	-1020.06
115.0	-4163.39	-3502.61	5171.27	-907.51
117.5	-4420.56	-3620.20	5436.39	-789.79
120.0	-4702.07	-3744.19	5726.12	-665.68
122.5	-5012.22	-3876.03	6044.82	-533.71
125.0	-5356.39	-4017.49	6397.87	-392.11
127.5	-5741.34	-4170.81	6792.12	-238.65
130.0	-6175.78	-4338.80	7236.33	-70.51
132.5	-6671.10	-4525.12	7741.97	115.98
135.0	-7242.48	-4734.61	8324.36	325.65
137.5	-7910.71	-4973.88	9004.47	565.11
140.0	-8705.01	-5252.14	9811.77	843.60
142.5	-9667.80	-5582.8	10789.17	1174.49
145.0	-10863.26	-5985.9	12001.73	1577.92
147.5	-12393.07	-6493.3	13553.46	2085.72
150.0	-14419.27	-7153.8	15630.88	2746.66

Appendix A.4 – Link 6,
Dynamic

R22: (mm)	F16X: (N)	F16Y: (N)	F56X: (N)	F56Y: (N)
75.0	-618.87	-3649.21	618.87	3796.36
77.5	-121.47	-2887.33	121.47	3034.48
80.0	155.04	-2487.99	-155.04	2635.14
82.5	344.78	-2224.60	-344.78	2371.75
85.0	489.51	-2030.64	-489.51	2177.79
87.5	607.37	-1877.81	-607.37	2024.96
90.0	707.74	-1751.75	-707.74	1898.90
92.5	796.11	-1644.23	-796.11	1791.38
95.0	875.92	-1550.13	-875.92	1697.28
97.5	949.49	-1466.05	-949.49	1613.20
100.0	1018.46	-1389.60	-1018.46	1536.75
102.5	1083.99	-1319.05	-1083.99	1466.20
105.0	1146.96	-1253.07	-1146.96	1400.22
107.5	1208.00	-1190.59	-1208.00	1337.74
110.0	1267.55	-1130.75	-1267.55	1277.90
112.5	1263.07	-1016.97	-1263.07	1164.12
115.0	1320.59	-965.31	-1320.59	1112.46
117.5	1377.03	-913.94	-1377.03	1061.09
120.0	1431.94	-862.31	-1431.94	1009.46
122.5	1484.46	-809.83	-1484.46	956.98
125.0	1533.11	-755.88	-1533.11	903.03
127.5	1575.40	-699.72	-1575.40	846.87
130.0	1607.31	-640.47	-1607.31	787.62
132.5	1622.21	-576.94	-1622.21	724.09
135.0	1609.16	-507.36	-1609.16	654.51
137.5	1549.83	-428.88	-1549.83	576.03
140.0	1413.03	-336.26	-1413.03	483.41
142.5	1145.07	-218.94	-1145.07	366.09
145.0	653.62	-53.75	-653.62	200.90
147.5	-216.98	213.31	216.98	-66.16
150.0	-1698.13	705.73	1698.13	-558.58

Appendix A.5 – F14, FP,
Dynamic

R22: (mm)	F14X: (N)	F14Y: (N)	FPX: (N)	FPY: (N)	FP(tangential): (N)
75.0	-1466.71	-1521.92	3309.86	882.16	314.59
77.5	-1638.97	-1699.11	2936.37	297.21	354.29
80.0	-1788.24	-1844.80	2790.00	43.32	374.62
82.5	-1934.87	-1981.42	2732.54	-83.67	383.76
85.0	-2081.68	-2111.78	2722.72	-147.49	386.71
87.5	-2230.31	-2237.35	2743.16	-174.94	385.86
90.0	-2382.07	-2359.19	2785.31	-179.37	382.48
92.5	-2538.09	-2478.13	2844.58	-168.15	377.31
95.0	-2699.49	-2594.92	2918.43	-145.67	370.84
97.5	-2867.39	-2710.26	3005.57	-114.64	363.37
100.0	-3042.98	-2824.80	3105.46	-76.76	355.13
102.5	-3227.56	-2939.21	3218.15	-33.15	346.28
105.0	-3422.55	-3054.15	3344.15	15.57	336.93
107.5	-3629.58	-3170.36	3484.42	69.02	327.16
110.0	-3850.48	-3288.58	3640.31	127.12	317.05
112.5	-3927.06	-3272.47	3665.10	193.57	283.76
115.0	-4163.39	-3384.89	3851.52	254.49	277.83
117.5	-4420.56	-3502.48	4060.12	320.88	271.45
120.0	-4702.07	-3626.47	4294.87	393.40	264.62
122.5	-5012.22	-3758.31	4560.96	472.93	257.31
125.0	-5356.39	-3899.77	4865.30	560.63	249.51
127.5	-5741.34	-4053.09	5217.18	657.99	241.17
130.0	-6175.78	-4221.08	5629.40	766.94	232.23
132.5	-6671.10	-4407.40	6120.07	889.95	222.63
135.0	-7242.48	-4616.89	6715.44	1030.13	212.26
137.5	-7910.71	-4856.16	7454.80	1191.20	201.01
140.0	-8705.01	-5134.42	8398.81	1377.17	188.78
142.5	-9667.80	-5465.04	9644.09	1590.86	175.48
145.0	-10863.26	-5868.17	11348.01	1829.25	161.21
147.5	-12393.07	-6375.61	13770.22	2070.16	146.50
150.0	-14419.27	-7036.10	17328.66	2238.89	135.67

Appendix B.1 – External Forces, Static

R22: (mm)	Actuator Force: (N)	Spring Force: (N)
75.0	0.00	0.00
77.5	50.00	-1.25
80.0	70.71	-2.50
82.5	86.60	-3.75
85.0	100.00	-5.00
87.5	111.80	-6.25
90.0	122.47	-7.50
92.5	132.29	-8.75
95.0	141.42	-10.00
97.5	150.00	-11.25
100.0	158.11	-12.50
102.5	165.83	-13.75
105.0	173.21	-15.00
107.5	180.28	-16.25
110.0	187.08	-17.50
112.5	193.65	-18.75
115.0	187.08	-20.00
117.5	180.28	-21.25
120.0	173.21	-22.50
122.5	165.83	-23.75
125.0	158.11	-25.00
127.5	150.00	-26.25
130.0	141.42	-27.50
132.5	132.29	-28.75
135.0	122.47	-30.00
137.5	111.80	-31.25
140.0	100.00	-32.50
142.5	86.60	-33.75
145.0	70.71	-35.00
147.5	50.00	-36.25
150.0	0.00	-37.50

Appendix B.2 Static

R22: (mm)	F12X: (N)	F12Y: (N)	F23X: (N)	F23Y: (N)
75.0	-1200	4800	-1200.00	4750.95
77.5	-1200	4800	-1151.25	4750.95
80.0	-1200	4800	-1131.79	4750.95
82.5	-1200	4800	-1117.15	4750.95
85.0	-1200	4800	-1105.00	4750.95
87.5	-1200	4800	-1094.45	4750.95
90.0	-1200	4800	-1085.03	4750.95
92.5	-1200	4800	-1076.46	4750.95
95.0	-1200	4800	-1068.58	4750.95
97.5	-1200	4800	-1061.25	4750.95
100.0	-1200	4800	-1054.39	4750.95
102.5	-1200	4800	-1047.92	4750.95
105.0	-1200	4800	-1041.79	4750.95
107.5	-1200	4800	-1035.97	4750.95
110.0	-1200	4800	-1030.42	4750.95
112.5	-1200	4800	-1025.10	4750.95
115.0	-1200	4800	-1032.92	4750.95
117.5	-1200	4800	-1040.97	4750.95
120.0	-1200	4800	-1049.29	4750.95
122.5	-1200	4800	-1057.92	4750.95
125.0	-1200	4800	-1066.89	4750.95
127.5	-1200	4800	-1076.25	4750.95
130.0	-1200	4800	-1086.08	4750.95
132.5	-1200	4800	-1096.46	4750.95
135.0	-1200	4800	-1107.53	4750.95
137.5	-1200	4800	-1119.45	4750.95
140.0	-1200	4800	-1132.50	4750.95
142.5	-1200	4800	-1147.15	4750.95
145.0	-1200	4800	-1164.29	4750.95
147.5	-1200	4800	-1186.25	4750.95
150.0	-1200	4800	-1237.50	4750.95

Appendix B.3 – Link 3,
Static

R22: (mm)	F43X: (N)	F43Y: (N)	F53X: (N)	F53Y: (N)
75.0	-1438.40	-1608.20	2638.40	-2897.50
77.5	-1607.64	-1782.44	2758.89	-2723.26
80.0	-1753.92	-1925.30	2885.71	-2580.40
82.5	-1897.55	-2059.21	3014.70	-2446.49
85.0	-2041.34	-2186.94	3146.34	-2318.76
87.5	-2186.92	-2309.97	3281.36	-2195.73
90.0	-2335.54	-2429.32	3420.57	-2076.38
92.5	-2488.35	-2545.84	3564.81	-1959.86
95.0	-2646.42	-2660.24	3715.00	-1845.46
97.5	-2810.86	-2773.20	3872.11	-1732.50
100.0	-2982.84	-2885.39	4037.22	-1620.31
102.5	-3163.61	-2997.44	4211.53	-1508.26
105.0	-3354.59	-3110.02	4396.39	-1395.68
107.5	-3557.35	-3223.84	4593.32	-1281.86
110.0	-3773.71	-3339.63	4804.12	-1166.07
112.5	-4005.77	-3458.23	5030.87	-1047.47
115.0	-4247.41	-3573.31	5280.32	-932.39
117.5	-4510.32	-3693.67	5551.29	-812.03
120.0	-4798.08	-3820.55	5847.37	-685.15
122.5	-5115.09	-3955.43	6173.01	-550.27
125.0	-5466.84	-4100.13	6533.73	-405.57
127.5	-5860.24	-4256.92	6936.49	-248.78
130.0	-6304.17	-4428.69	7390.25	-77.01
132.5	-6810.28	-4619.16	7906.74	113.46
135.0	-7394.08	-4833.29	8501.60	327.59
137.5	-8076.79	-5077.80	9196.23	572.10
140.0	-8888.24	-5362.13	10020.74	856.43
142.5	-9871.78	-5699.91	11018.93	1194.21
145.0	-11092.93	-6111.72	12257.22	1606.02
147.5	-12655.55	-6630.02	13841.80	2124.32
150.0	-14725.35	-7304.71	15962.85	2799.01

Appendix B.4 – Link 6,
Static

R22: (mm)	F16X: (N)	F16Y: (N)	F56X: (N)	F56Y: (N)
75.0	-607.99	-3568.81	607.99	3715.96
77.5	-119.88	-2822.30	119.88	2969.45
80.0	151.06	-2430.95	-151.06	2578.10
82.5	336.79	-2172.77	-336.79	2319.92
85.0	478.36	-1982.62	-478.36	2129.77
87.5	593.56	-1832.79	-593.56	1979.94
90.0	691.61	-1709.20	-691.61	1856.35
92.5	777.87	-1603.78	-777.87	1750.93
95.0	855.74	-1511.51	-855.74	1658.66
97.5	927.48	-1429.07	-927.48	1576.22
100.0	994.68	-1354.11	-994.68	1501.26
102.5	1058.50	-1284.92	-1058.50	1432.07
105.0	1119.77	-1220.20	-1119.77	1367.35
107.5	1179.12	-1158.91	-1179.12	1306.06
110.0	1236.96	-1100.19	-1236.96	1247.34
112.5	1293.55	-1043.31	-1293.55	1190.46
115.0	1352.41	-990.54	-1352.41	1137.69
117.5	1410.20	-938.06	-1410.20	1085.21
120.0	1466.47	-885.31	-1466.47	1032.46
122.5	1520.35	-831.69	-1520.35	978.84
125.0	1570.31	-776.57	-1570.31	923.72
127.5	1613.85	-719.20	-1613.85	866.35
130.0	1646.86	-658.67	-1646.86	805.82
132.5	1662.60	-593.77	-1662.60	740.92
135.0	1649.92	-522.73	-1649.92	669.88
137.5	1590.15	-442.63	-1590.15	589.78
140.0	1451.47	-348.18	-1451.47	495.33
142.5	1179.13	-228.66	-1179.13	375.81
145.0	678.88	-60.54	-678.88	207.69
147.5	-208.20	211.07	208.20	-63.92
150.0	-1718.77	711.99	1718.77	-564.84

Appendix B.5 – F14, FP,
Static

R22: (mm)	F14X: (N)	F14Y: (N)	FPX: (N)	FPY: (N)	FP(tangential): (N)
75.0	-1438.40	-1490.48	3246.39	867.51	306.43
77.5	-1607.64	-1664.72	2878.77	295.24	343.58
80.0	-1753.92	-1807.58	2734.65	46.75	362.94
82.5	-1897.55	-1941.49	2677.90	-77.52	371.64
85.0	-2041.34	-2069.22	2667.98	-139.94	374.37
87.5	-2186.92	-2192.25	2687.80	-166.74	373.41
90.0	-2335.54	-2311.60	2728.96	-170.98	369.99
92.5	-2488.35	-2428.12	2786.94	-159.89	364.82
95.0	-2646.42	-2542.52	2859.26	-137.75	358.37
97.5	-2810.86	-2655.48	2944.63	-107.23	350.94
100.0	-2982.84	-2767.67	3042.54	-70.00	342.75
102.5	-3163.61	-2879.72	3153.04	-27.14	333.96
105.0	-3354.59	-2992.30	3276.62	20.73	324.68
107.5	-3557.35	-3106.12	3414.21	73.25	314.99
110.0	-3773.71	-3221.91	3567.16	130.32	304.97
112.5	-4005.77	-3340.51	3737.32	192.04	294.65
115.0	-4247.41	-3455.59	3927.91	254.35	288.48
117.5	-4510.32	-3575.95	4141.09	322.24	281.86
120.0	-4798.08	-3702.83	4380.90	396.36	274.78
122.5	-5115.09	-3837.71	4652.67	477.62	267.24
125.0	-5466.84	-3982.41	4963.41	567.20	259.21
127.5	-5860.24	-4139.20	5322.63	666.62	250.64
130.0	-6304.17	-4310.97	5743.39	777.86	241.48
132.5	-6810.28	-4501.44	6244.14	903.43	231.63
135.0	-7394.08	-4715.57	6851.68	1046.52	221.00
137.5	-8076.79	-4960.08	7606.08	1210.93	209.45
140.0	-8888.24	-5244.41	8569.26	1400.81	196.84
142.5	-9871.78	-5582.19	9839.80	1619.07	183.04
145.0	-11092.93	-5994.00	11578.34	1862.76	168.04
147.5	-12655.55	-6512.30	14050.00	2109.44	152.22
150.0	-14725.35	-7186.99	17681.62	2283.22	139.68

Appendix C.1 – ΣA
Equation of Motion

R22: (mm)	ΣA : kg
75.0	445.40
77.5	369.81
80.0	338.38
82.5	321.12
85.0	310.28
87.5	302.97
90.0	297.85
92.5	294.22
95.0	291.66
97.5	289.94
100.0	288.89
102.5	288.41
105.0	288.42
107.5	288.88
110.0	289.77
112.5	291.08
115.0	292.80
117.5	294.97
120.0	297.60
122.5	300.76
125.0	304.51
127.5	308.97
130.0	314.27
132.5	320.66
135.0	328.48
137.5	338.29
140.0	351.02
142.5	368.32
145.0	393.21
147.5	431.22
150.0	491.76

```
%ME 352 - LAB PROJECT 2 - SIX-BAR LINKAGE - ELENA HELVAJIAN
```

```
clear
clc
```

```
%GIVEN VALUES
```

```
%LENGTH
```

```
g = 9.81; %m/s^2
R1 = 150; %mms
R3 = 75; %mms
R33 = 212.5; %mms
R4 = 100; %mms
R5 = 150; %mms
R6 = 62.5; %mms
BC = 150; %mms
CP = 150; %mms
rho = 12.5; %mms
R11 = 185; %mm
Rs = 110; %mm
```

```
%MASS
```

```
m2 = 5; %kg
m3 = 25; %kg
m4 = 12; %kg
m5 = 5; %kg
m6 = 15; %kg
```

```
%MASS MOMENTS OF INERTIA
```

```
IG2 = 30; %N*mm-s^2
IG3 = 450; %N*mm-s^2
IG4 = 75; %N*mm-s^2
IG5 = 250; %N*mm-s^2
IG6 = 20; %N*mm-s^2
```

```
%OTHER
```

```
T12 = 15; %kN*m
C = 2000; %N*sec/m
mu = 0.25;
k = 500; %N/m
```

```
%ANGLE
```

```
alpha = acos((150^2+212.5^2-75^2)/(2*212.5*150))*180/pi; %rads (Angle between AC and AB)
beta = acos((150^2+75^2-212.5^2)/(2*150*75)); %rads (Angle between AB and BC)
theta_1 = 0; %rads
theta_2 = 0; %rads
theta_22 = 0; %rads
theta_3_guess = 96.38/180*pi; %rads (original guess for Theta 3)
theta_4_guess = 228.19/180*pi; %rads (original guess for Theta 4)
theta_5_guess = 229.94/180*pi; %rads (original guess for Theta 5)
theta_6_guess = 260.7/180*pi; %rads (original guess for Theta 6)
theta_2_prime = -1 / rho; % (rad/mm)
theta_2_2prime = 0; % (rad/mm^2)
```

```
%ADDITIONAL INFORMATION
```

```
tol = 0.01/180*pi; %tolerance in radians
```

```
%ACCELERATION
```

```
R_doubledot_22 = 0.125; %m/s^2
```

```
%INITIALIZE VECTORS
R22all = []; %mms
theta_3all = []; %rads
theta_4all = []; %rads
theta_5all = []; %rads
theta_6all = []; %rads
theta_3_primeall = []; %mm/mm
theta_4_primeall = []; %mm/mm
theta_5_primeall = []; %mm/mm
theta_6_primeall = []; %mm/mm
theta_3_2primeall = []; %mm/mm^2
theta_4_2primeall = []; %mm/mm^2
theta_5_2primeall = []; %mm/mm^2
theta_6_2primeall = []; %mm/mm^2
omega_2all = []; %rad/s
omega_3all = []; %rad/s
omega_4all = []; %rad/s
omega_5all = []; %rad/s
omega_6all = []; %rad/s
accel_2all = []; %rad/s^2
accel_3all = []; %rad/s^2
accel_4all = []; %rad/s^2
accel_5all = []; %rad/s^2
accel_6all = []; %rad/s^2
Xp_all = []; %mms
Yp_all = []; %mms
Xp_primeall = []; %mm/mm
Yp_primeall = []; %mm/mm
Xp_2primeall = []; %mm/mm^2
Yp_2primeall = []; %mm/mm^2
Ut_X_all = []; %no units
Ut_Y_all = []; %no units
Un_X_all = []; %no units
Un_Y_all = []; %no units
rho_c_all = []; %mms
Xcc_all = []; %mms
Ycc_all = []; %mms
Vp_X_all = []; %mm/s
Vp_Y_all = []; %mm/s
Ap_X_all = []; %mm/s^2
Ap_Y_all = []; %mm/s^2
theta_2primeall = []; %mm/mm
F5x_all = [];
F5y_all = [];
Ffric_all = [];
F19X_all = [];
F29X_all = [];
F18X_all = [];
F28X_all = [];
AG3x_all = [];
AG3y_all = [];
AG5x_all = [];
AG5y_all = [];
F12X_all = [];
F12Y_all = [];
F14X_all = [];
F14Y_all = [];
```

```

F16X_all = [];
F16Y_all = [];
F23X_all = [];
F23Y_all = [];
F34X_all = [];
F34Y_all = [];
F35X_all = [];
F35Y_all = [];
F56X_all = [];
F56Y_all = [];
FPX_all = [];
FPY_all = [];
FP_all = [];
FP_tanXall = [];
FP_tanYall = [];
rdot_all = [];
Fp_tanall = [];
F12XS_all = [];
F12YS_all = [];
F18XS_all = [];
F19XS_all = [];
F28XS_all = [];
F29XS_all = [];
F82XS_all = [];
F92XS_all = [];
F23XS_all = [];
F23YS_all = [];
F34XS_all = [];
F34YS_all = [];
F14XS_all = [];
F14YS_all = [];
F35XS_all = [];
F35YS_all = [];
F56XS_all = [];
F56YS_all = [];
F16XS_all = [];
F16YS_all = [];
FPXS_all = [];
FPYS_all = [];
FPS_tanall = [];
FPS_all = [];
Asum_all = [];
Fp_power_tan_all = [];

```

%CALCULATIONS

```
for R22 = 75:.1:150
```

```
    R22all = [R22all,R22]; %mms (All R22 values in this vector)
```

% CALCULATE THETA 3 AND 4 USING NEWTON RAPHSON

```

ex = R4*cos(theta_4_guess)+R3*cos(theta_3_guess) + R22*cos(theta_22);
ey = R4*sin(theta_4_guess)+R3*sin(theta_3_guess) + R22*sin(theta_22);
a11 = -R3*sin(theta_3_guess);
a12 = -R4*sin(theta_4_guess);
a21 = R3*cos(theta_3_guess);
a22 = R4*cos(theta_4_guess);

```

```
determinant1 = (a11*a22)-(a21*a12);
```

```

    delta_theta_3 = (-ex*a22-(-ey)*a12)/determinant1; %value the guess of Theta 3 needs
to change by
    delta_theta_4 = (-ey*a11-(-ex)*a21)/determinant1; %value the guess of Theta 4 needs
to change by

while abs(delta_theta_3) > tol || abs(delta_theta_4) > tol
    ex = R4*cos(theta_4_guess)+R3*cos(theta_3_guess) + R22*cos(theta_22);
    ey = R4*sin(theta_4_guess)+R3*sin(theta_3_guess) + R22*sin(theta_22);
    a11 = -R3*sin(theta_3_guess);
    a12 = -R4*sin(theta_4_guess);
    a21 = R3*cos(theta_3_guess);
    a22 = R4*cos(theta_4_guess);
    determinant1 = (a11*a22)-(a12*a21);

    delta_theta_3 = ((-ex*a22)-((-ey)*a12))/determinant1; %value the guess of Theta 3
needs to change by
    delta_theta_4 = ((-ey*a11)-((-ex)*a21))/determinant1; %value the guess of Theta 4
needs to change by
    theta_3_guess = (theta_3_guess + delta_theta_3); %rads (final value of Theta 3)
    theta_4_guess = (theta_4_guess + delta_theta_4); %rads (final value of Theta 4)
end

    theta_3all = [theta_3all, theta_3_guess*180/pi]; %rads (All Theta 3 values in this
vector)
    theta_4all = [theta_4all, theta_4_guess*180/pi]; %rads (All Theta 4 values in this
vector)

%CALCULATE FIRST-ORDER KINEMATIC COEFFICIENT FOR THETA 3 AND 4
b11 = -R3*sin(theta_3_guess);
b12 = -R4*sin(theta_4_guess);
b21 = R3*cos(theta_3_guess);
b22 = R4*cos(theta_4_guess);

val1 = -cos(theta_22);
val2 = -sin(theta_22);
determinant2 = (b11*b22)-(b12*b21);

theta_3_prime = ((val1 * b22) - (b12 * val2))/determinant2; %mm/mm
theta_4_prime = ((b11 * val2) - (val1 * b21))/determinant2; %mm/mm
theta_3_primeall = [theta_3_primeall,theta_3_prime]; %mm/mm (All Theta 3 Prime values
in this vector)
theta_4_primeall = [theta_4_primeall,theta_4_prime]; %mm/mm (All Theta 4 Prime values
in this vector)

%CALCULATE SECOND-ORDER KINEMATIC COEFFICIENT FOR THETA 3 AND 4
val3 = R3*cos(theta_3_guess)*(theta_3_prime^2) + R4*cos(theta_4_guess)*
(theta_4_prime^2);
val4 = R3*sin(theta_3_guess)*(theta_3_prime^2) + R4*sin(theta_4_guess)*
(theta_4_prime^2);
theta_3_2prime = ((val3 * b22) - (b12 * val4)) / determinant2; %mm/mm^2
theta_4_2prime = ((b11 * val4) - (val3 * b21)) / determinant2; %mm/mm^2
theta_3_2primeall = [theta_3_2primeall,theta_3_2prime]; %mm/mm^2 (All Theta 3 Double
Prime values in this vector)
theta_4_2primeall = [theta_4_2primeall,theta_4_2prime]; %mm/mm^2 (All Theta 4 Double
Prime values in this vector)

%CONSTRAINT FOR VLE #2 - UPDATE THE VALUE OF THETA 33
theta_33 = theta_3_guess + (27.47)/180*pi;

```

```

%CALCULATE THETA 5 AND 6 USING NEWTON RAPHSON
ex2 = R22*cos(theta_22)+R33*cos(theta_33)+R5*cos(theta_5_guess)+R6*cos(theta_6_guess) +R1*cos(theta_1);
ey2 = R22*sin(theta_22)+R33*sin(theta_33)+R5*sin(theta_5_guess)+R6*sin(theta_6_guess) +R1*sin(theta_1);
c11 = -R5*sin(theta_5_guess);
c12 = -R6*sin(theta_6_guess);
c21 = R5*cos(theta_5_guess);
c22 = R6*cos(theta_6_guess);

determinant3 = (c11*c22)-(c12*c21);
delta_theta_5 = (((-ex2)*c22)-((-ey2)*c12))/determinant3; %value the guess of Theta 5
needs to change by
delta_theta_6 = (((-ey2)*c11)-((-ex2)*c21))/determinant3; %value the guess of Theta 6
needs to change by

while abs(delta_theta_5) > tol || abs(delta_theta_6) > tol
    ex2 = R22*cos(theta_22)+R33*cos(theta_33)+R5*cos(theta_5_guess)+R6*cos(theta_6_guess)+R1*cos(theta_1);
    ey2 = R22*sin(theta_22)+R33*sin(theta_33)+R5*sin(theta_5_guess)+R6*sin(theta_6_guess)+R1*sin(theta_1);
    c11 = -R5*sin(theta_5_guess);
    c12 = -R6*sin(theta_6_guess);
    c21 = R5*cos(theta_5_guess);
    c22 = R5*cos(theta_6_guess);

    determinant3 = (c11*c22)-(c12*c21);
    delta_theta_5 = (((-ex2)*c22)-((-ey2)*c12))/determinant3; %value the guess of
Theta 5 needs to change by
    delta_theta_6 = (((-ey2)*c11)-((-ex2)*c21))/determinant3; %value the guess of
Theta 6 needs to change by
    theta_5_guess = theta_5_guess + delta_theta_5; %rads (final value of Theta 5)
    theta_6_guess = theta_6_guess + delta_theta_6; %rads (final value of Theta 6)
end

theta_5all = [theta_5all, theta_5_guess*180/pi]; %rads (All Theta 5 values in this
vector)
theta_6all = [theta_6all, theta_6_guess*180/pi]; %rads (All Theta 6 values in this
vector)

%CALCULATE FIRST-ORDER KINEMATIC COEFFICIENT FOR THETA 5 AND 6
d11 = -R5*sin(theta_5_guess);
d12 = -R6*sin(theta_6_guess);
d21 = R5*cos(theta_5_guess);
d22 = R6*cos(theta_6_guess);

val5 = -cos(theta_22) + R33*sin(theta_33)*theta_3_prime;
val6 = -sin(theta_22) - R33*cos(theta_33)*theta_3_prime;
determinant4 = (d11*d22) - (d12*d21);

theta_5_prime = ((val5 * d22) - (d12 * val6)) / determinant4; %mm/mm
theta_6_prime = ((d11 * val6) - (val5 * d21)) / determinant4; %mm/mm
theta_5_primeall = [theta_5_primeall,theta_5_prime]; %mm/mm (All Theta 5 Prime values
in this vector)
theta_6_primeall = [theta_6_primeall,theta_6_prime]; %mm/mm (All Theta 6 Prime values
in this vector)

```

```

%CALCULATE SECOND ORDER KINEMATIC COEFFICIENTS FOR THETA 3 AND 4
val7 = R33*cos(theta_33)*(theta_3_prime^2)+R33*sin(theta_33)*(theta_3_2prime)+R5*cos(
(theta_5_guess)*(theta_5_prime^2)+R6*cos(theta_6_guess)*(theta_6_prime^2);
val8 = R33*sin(theta_33)*(theta_3_prime^2)-R33*cos(theta_33)*(theta_3_2prime)+R5*sin(
(theta_5_guess)*(theta_5_prime^2)+R6*sin(theta_6_guess)*(theta_6_prime^2);
theta_5_2prime = ((val7 * d22) - (d12 * val8)) / determinant4; %mm/mm^2
theta_6_2prime = ((d11 * val8) - (val7 * d21)) / determinant4; %mm/mm^2
theta_5_2primeall = [theta_5_2primeall,theta_5_2prime]; %mm/mm^2 (All Theta 5 Double
Prime values in this vector)
theta_6_2primeall = [theta_6_2primeall,theta_6_2prime]; %mm/mm^2 (All Theta 6 Double
Prime values in this vector)

%CALCULATE OMEGA 2, 3, 4, 5, AND 6
if R22 < 112.5 %mm
    %Angular Velocity of all links when R22 is less than 112.5 mm
    omega_2 = -sqrt(2*R_doubledot_22*(R22/1000-0.075))*1000/rho;
    omega_3 = theta_3_prime*sqrt(2*R_doubledot_22*(R22/1000-0.075))*1000;
    omega_4 = theta_4_prime*sqrt(2*R_doubledot_22*(R22/1000-0.075))*1000;
    omega_5 = theta_5_prime*sqrt(2*R_doubledot_22*(R22/1000-0.075))*1000;
    omega_6 = theta_6_prime*sqrt(2*R_doubledot_22*(R22/1000-0.075))*1000;
    %Angular Acceleration of all links when R22 is less than 112.5 mm
    accel_2 = -R_doubledot_22*1000/rho;
    accel_3 = theta_3_2prime*(sqrt(2*R_doubledot_22*(R22/1000-0.075))*1000)
^2+theta_3_prime*R_doubledot_22*1000;
    accel_4 = theta_4_2prime*(sqrt(2*R_doubledot_22*(R22/1000-0.075))*1000)
^2+theta_4_prime*R_doubledot_22*1000;
    accel_5 = theta_5_2prime*(sqrt(2*R_doubledot_22*(R22/1000-0.075))*1000)
^2+theta_5_prime*R_doubledot_22*1000;
    accel_6 = theta_6_2prime*(sqrt(2*R_doubledot_22*(R22/1000-0.075))*1000)
^2+theta_6_prime*R_doubledot_22*1000;

    %Update Vectors
    omega_2all = [omega_2all,omega_2]; %rad/s
    omega_3all = [omega_3all,omega_3]; %rad/s
    omega_4all = [omega_4all,omega_4]; %rad/s
    omega_5all = [omega_5all,omega_5]; %rad/s
    omega_6all = [omega_6all,omega_6]; %rad/s
    accel_2all = [accel_2all,accel_2]; %rad/s^2
    accel_3all = [accel_3all,accel_3]; %rad/s^2
    accel_4all = [accel_4all,accel_4]; %rad/s^2
    accel_5all = [accel_5all,accel_5]; %rad/s^2
    accel_6all = [accel_6all,accel_6]; %rad/s^2
else
    %Angular Velocity of all links when R22 is greater than or equal to 112.5 mm
    omega_2 = -sqrt(2*-R_doubledot_22*(R22/1000-0.15))*1000/rho;
    omega_3 = theta_3_prime*sqrt(2*-R_doubledot_22*(R22/1000-0.15))*1000;
    omega_4 = theta_4_prime*sqrt(2*-R_doubledot_22*(R22/1000-0.15))*1000;
    omega_5 = theta_5_prime*sqrt(2*-R_doubledot_22*(R22/1000-0.15))*1000;
    omega_6 = theta_6_prime*sqrt(2*-R_doubledot_22*(R22/1000-0.15))*1000;
    %Angular Acceleration of all links when R22 is greater than or equal to 112.5 mm
    accel_2 = R_doubledot_22*1000/rho;
    accel_3 = theta_3_2prime*(sqrt(2*-R_doubledot_22*(R22/1000-0.15))*1000)
^2+theta_3_prime*-R_doubledot_22*1000;
    accel_4 = theta_4_2prime*(sqrt(2*-R_doubledot_22*(R22/1000-0.15))*1000)
^2+theta_4_prime*-R_doubledot_22*1000;
    accel_5 = theta_5_2prime*(sqrt(2*-R_doubledot_22*(R22/1000-0.15))*1000)
^2+theta_5_prime*-R_doubledot_22*1000;
    accel_6 = theta_6_2prime*(sqrt(2*-R_doubledot_22*(R22/1000-0.15))*1000)
^2+theta_6_prime*-R_doubledot_22*1000;

```



```

^2+theta_6_prime*-R_doubledot_22*1000;

%Update Vectors
omega_2all = [omega_2all,omega_2]; %rad/s
omega_3all = [omega_3all,omega_3]; %rad/s
omega_4all = [omega_4all,omega_4]; %rad/s
omega_5all = [omega_5all,omega_5]; %rad/s
omega_6all = [omega_6all,omega_6]; %rad/s
accel_2all = [accel_2all,accel_2]; %rad/s^2
accel_3all = [accel_3all,accel_3]; %rad/s^2
accel_4all = [accel_4all,accel_4]; %rad/s^2
accel_5all = [accel_5all,accel_5]; %rad/s^2
accel_6all = [accel_6all,accel_6]; %rad/s^2
end

%ANALYSIS OF POINT P
%POSITION OF P
Xp = -2*R5*cos(theta_5_guess)-R6*cos(theta_6_guess); %position of point P in the
X direction (mms)
Yp = -2*R5*sin(theta_5_guess)-R6*sin(theta_6_guess); %position of point P in the
Y direction (mms)

%FIRST-ORDER KINEMATIC COEFFICIENT
Xp_prime = 2*R5*sin(theta_5_guess)*theta_5_prime+R6*sin(theta_6_guess)
*theta_6_prime;
Yp_prime = -2*R5*cos(theta_5_guess)*theta_5_prime-R6*cos(theta_6_guess)
*theta_6_prime;

%SECOND-ORDER KINEMATIC COEFFICIENT
Xp_2prime = 2*R5*cos(theta_5_guess)*((theta_5_prime)^2)+2*R5*sin(theta_5_guess)
*theta_5_2prime+R6*cos(theta_6_guess)*((theta_6_prime)^2)+R6*sin(theta_6_guess)
(theta_6_2prime);
Yp_2prime = 2*R5*sin(theta_5_guess)*((theta_5_prime)^2)-2*R5*cos(theta_5_guess)
*theta_5_2prime+R6*sin(theta_6_guess)*((theta_6_prime)^2)-R6*cos(theta_6_guess)
*theta_6_2prime;

%CALCULATE RADIUS OF CURVATURE AND CENTER OF CURVATURE
Rp_prime = sqrt(Xp_prime^2+Yp_prime^2);
rho_c = Rp_prime^3/(Xp_prime*Yp_2prime- Xp_2prime*Yp_prime);
Ut_X = Xp_prime/Rp_prime; %Unit Tangent in the X direction
Ut_Y = Yp_prime/Rp_prime; %Unit Tangent in the Y direction
Un_X = -Yp_prime/Rp_prime; %Unit Normal in the X direction
Un_Y = Xp_prime/Rp_prime; %Unit Normal in the Y direction
Xcc = Xp + rho_c*Un_X;
Ycc = Yp + rho_c*Un_Y;

%Update Vectors
Xp_all = [Xp_all,Xp]; %mms (All Xp values in this vector)
Yp_all = [Yp_all,Yp]; %mms (All Yp values in this vector)
Xp_primeall = [Xp_primeall,Xp_prime]; %mm/mm (All Xp Prime values in this vector)
Yp_primeall = [Yp_primeall,Yp_prime]; %mm/mm (All Yp Prime values in this vector)
Xp_2primeall = [Xp_2primeall,Xp_2prime]; %mm/mm^2 (All Xp Double Prime values in this
vector)
Yp_2primeall = [Yp_2primeall,Yp_2prime]; %mm/mm^2 (All Yp Double Prime values in this
vector)
Ut_X_all = [Ut_X_all,Ut_X]; %no units (Unit Tangent in the X direction)
Un_X_all = [Un_X_all,Un_X]; %no units (Unit Tangent in the Y direction)
Ut_Y_all = [Ut_Y_all,Ut_Y]; %no units (Unit Normal in the X direction)

```

```

Un_Y_all = [Un_Y_all,Un_Y]; %no units (Unit Normal in the Y direction)
rho_c_all = [rho_c_all,rho_c]; %mms (All Radius of Curvature values in this vector)
Xcc_all = [Xcc_all,Xcc]; %mms (All Center of Curvature position values in the X
direction in this vector)
Ycc_all = [Ycc_all,Ycc]; %mms (All Center of Curvature position values in the Y
direction in this vector)

if R22 < 112.5
    R_dd22 = R_doubledot_22;
    Vp_X = Xp_prime*sqrt(2*R_doubledot_22*(R22/1000-0.075))*1000; %mm/s (Velocity of
Point P in the X direction when R22 is greater than 112.5 mm)
    Vp_Y = Yp_prime*sqrt(2*R_doubledot_22*(R22/1000-0.075))*1000; %mm/s (Velocity of
Point P in the Y direction when R22 is greater than 112.5 mm)
    r_dot = sqrt(2*R_doubledot_22*(R22/1000-0.075))*1000; %mm/s
    Ap_X = 100*Xp_2prime*(r_dot)^2+Xp_prime*R_doubledot_22*1000; %mm/s^2
(Acceleration of Point P in the X direction when R22 is greater than 112.5 mm)
    Ap_Y = 100*Yp_2prime*(r_dot)^2+Yp_prime*R_doubledot_22*1000; %mm/s^2
(Acceleration of Point P in the Y direction when R22 is greater than 112.5 mm)

else
    R_dd22 = -R_doubledot_22;
    Vp_X = Xp_prime*sqrt(2*-R_doubledot_22*(R22/1000-0.15))*1000; %mm/s (Velocity of
Point P in the X direction when R22 is greater than 112.5 mm)
    Vp_Y = Yp_prime*sqrt(2*-R_doubledot_22*(R22/1000-0.15))*1000; %mm/s (Velocity of
Point P in the Y direction when R22 is greater than 112.5 mm)
    r_dot = sqrt(2*-R_doubledot_22*(R22/1000-0.15))*1000; %mm/s
    Ap_X = 100*Xp_2prime*(r_dot)^2+Xp_prime*-R_doubledot_22*1000; %mm/s^2
(Acceleration of Point P in the X direction when R22 is greater than 112.5 mm)
    Ap_Y = 100*Yp_2prime*(r_dot)^2+Yp_prime*-R_doubledot_22*1000; %mm/s^2
(Acceleration of Point P in the Y direction when R22 is greater than 112.5 mm)

end
rdot_all = [rdot_all,r_dot];

%Update Vectors
Vp_X_all = [Vp_X_all,Vp_X]; %mm/s (Velocity of Point P in the X direction)
Vp_Y_all = [Vp_Y_all,Vp_Y]; %mm/s (Velocity of Point P in the Y direction)
Ap_X_all = [Ap_X_all,Ap_X]; %mm/s^2 (Acceleration of Point P in the X direction)
Ap_Y_all = [Ap_Y_all,Ap_Y]; %mm/s^2 (Acceleration of Point P in the Y direction)

RG3x = -R4*cos(theta_4_guess)+R1*cos(theta_1);
RG3y = -R4*sin(theta_4_guess)+R1*sin(theta_1);
RG3x_prime = R4*sin(theta_4_guess)*theta_4_prime;%rads
RG3y_prime = -R4*cos(theta_4_guess)*theta_4_prime;
RG3x_2prime = R4*cos(theta_4_guess)*(theta_4_prime)^2+R4*sin(theta_4_guess)
*theta_4_2prime;%rad/mm
RG3y_2prime = R4*sin(theta_4_guess)*(theta_4_prime)^2-R4*cos(theta_4_guess)
*theta_4_2prime;%rad/mm

AG3x = (RG3x_prime*R_dd22*1000+RG3x_2prime*(r_dot)^2); %mm/s^2
AG3y = (RG3y_prime*R_dd22*1000+RG3y_2prime*(r_dot)^2); %mm/s^2

RG5x = -R5*cos(theta_5_guess)-R6*cos(theta_6_guess);
RG5y = -R5*sin(theta_5_guess)-R6*sin(theta_6_guess);
RG5x_prime = R5*sin(theta_5_guess)*theta_5_prime+R6*sin(theta_6_guess)*theta_6_prime;
RG5y_prime = -R5*cos(theta_5_guess)*theta_5_prime-R6*cos(theta_6_guess)
*theta_6_prime;
RG5x_2prime = R5*cos(theta_5_guess)*(theta_5_prime)^2+R5*sin(theta_5_guess)

```

```
*theta_5_2prime+R6*cos(theta_6_guess)*(theta_6_prime)^2+R6*sin(theta_6_guess)↵
*theta_6_2prime;
  RG5y_2prime = R5*sin(theta_5_guess)*(theta_5_prime)^2-R5*cos(theta_5_guess)↵
*theta_5_2prime+R6*sin(theta_6_guess)*(theta_6_prime)^2-R6*cos(theta_6_guess)↵
*theta_6_2prime;
```

```
AG5x = (RG5x_prime*R_dd22*1000+RG5x_2prime*(r_dot)^2); %mm/s^2
AG5y = (RG5y_prime*R_dd22*1000+RG5y_2prime*(r_dot)^2); %mm/s^2
```

```
AG3x_all = [AG3x_all,AG3x];
AG3y_all = [AG3y_all,AG3y];
AG5x_all = [AG5x_all,AG5x];
AG5y_all = [AG5y_all,AG5y];
```

%DYNAMIC FORCE ANALYSIS

%LINK 9 AND 8

```
F19X = C*r_dot/1000;
F18X = k*(R11-R22-Rs)/1000;
```

```
F19X_all = [F19X_all,F19X];
F18X_all = [F18X_all,F18X];
```

```
F28X = -F18X;
F29X = -F19X;
F82X = -F28X;
F92X = -F29X;
```

```
F28X_all = [F28X_all,F28X];
F29X_all = [F29X_all,F29X];
```

%LINK 2

```
F12X = (IG2*accel_2-T12*1000)/(rho);
F12Y = abs(F12X)/mu;
```

```
F12X_all = [F12X_all,F12X];
F12Y_all = [F12Y_all,F12Y];
```

```
F32X = m2*R_dd22 + F29X + F28X - F12X;
F32Y = m2*g-F12Y;
```

%LINK 3

%POSITION AND CHANGE IN POSITION VALUES FOR LINK 3

```
R3X = R3*cos(theta_3_guess);
R3Y = R3*sin(theta_3_guess);
R33X = -R33*cos(theta_33);
R33Y = -R33*sin(theta_33);
R333X = -BC*cos(theta_3_guess+40.804/180*pi);
R333Y = -BC*sin(theta_3_guess+40.804/180*pi);
R4X = -R4*cos(theta_4_guess);
R4Y = -R4*sin(theta_4_guess);
R5X = -R5*cos(theta_5_guess);
R5Y = -R5*sin(theta_5_guess);
R6X = -R6*cos(theta_6_guess);
R6Y = -R6*sin(theta_6_guess);
```

```
F23X = -F32X;
F23Y = -F32Y;
```

```

% SOLVE FOR F34X AND F34Y
e11 = -R333X;
e12 = R333Y;
e21 = R4X;
e22 = -R4Y;

ot1 = IG3*accel_3 + m3*(R333X*AG3y-R333Y*AG3x)/1000 + R333X*g*m3 - (R333X*F23Y-
R333Y*F23X);
ot2 = IG4*accel_4;
determinant5 = (e11*e22) - (e12*e21);

F34Y = ((ot1 * e22) - (e12 * ot2)) / determinant5; %mm/mm
F34X = ((e11 * ot2) - (ot1 * e21)) / determinant5; %mm/mm

F43X = -F34X;
F43Y = -F34Y;

F53X = m3*AG3x/1000-F23X-F43X;
F53Y = m3*AG3y/1000-F23Y-F43Y+m3*g;

F35X = -F53X;
F35Y = -F53Y;

%LINK 4
F14X = -F34X;
F14Y = m4*g - F34Y;

%LINK 5
% SOLVE FOR F65X AND F65Y
f11 = -2*R5Y;
f12 = 2*R5X;
f21 = R6Y;
f22 = -R6X;

ot3 = IG5*accel_5 + m5*(R5X*AG5y-R5Y*AG5x)/1000 + R5X*g*m5 - (R5X*F35Y-R5Y*F35X);
ot4 = IG6*accel_6;
determinant6 = (f11*f22) - (f12*f21);

F65X = ((ot3 * f22) - (f12 * ot4)) / determinant6; %N
F65Y = ((f11 * ot4) - (ot3 * f21)) / determinant6; %N
F56X = -F65X;
F56Y = -F65Y;

%LINK 6
F16X = -F56X;
F16Y = m6*g-F56Y;

%SOLVE FOR FP
theta_p = atan((m5*AG5y/1000+m5*g-F65Y-F35Y)/(m5*AG5x/1000-F35X-F65X))*180/pi;
FPX = m5*AG5x/1000-F35X-F65X;
FPY = m5*AG5y/1000-F35Y-F65Y + m5*g;
FP = sqrt(FPX^2+FPY^2);

%SOLVE FOR TANGENT OF FP
FpX_tan = Ut_X*FPX;
FpY_tan = Ut_Y*FPY;
Fptan = FpX_tan + FpY_tan;

```

%UPDATE ALL VECTORS

```

F14X_all = [F14X_all,F14X];
F14Y_all = [F14Y_all,F14Y];
F16X_all = [F16X_all,F16X];
F16Y_all = [F16Y_all,F16Y];
F23X_all = [F23X_all,F23X];
F23Y_all = [F23Y_all,F23Y];
F34X_all = [F34X_all,F34X];
F34Y_all = [F34Y_all,F34Y];
F35X_all = [F35X_all,F35X];
F35Y_all = [F35Y_all,F35Y];
F56X_all = [F56X_all,F56X];
F56Y_all = [F56Y_all,F56Y];
FPX_all = [FPX_all,FPX];
FPY_all = [FPY_all,FPY];
FP_all = [FP_all,FP];
FP_tanXall = [FP_tanXall,FpX_tan];
FP_tanYall = [FP_tanYall,FpY_tan];
Fp_tanall = [Fp_tanall,Fptan];

```

%STATIC FORCE ANALYSIS

%LINK 8

```

F18XS = F18X;
F28XS = F28X;
F82XS = -F28XS;

```

%LINK 9

```

F19XS = F19X;
F29XS = F29X;
F92XS = -F29XS;

```

%LINK 2

```

F12XS = T12/-rho*1000; %N
F12YS = abs(F12XS/mu);

```

```

F32XS = -F12XS -F82XS -F92XS;
F32YS = m2*g - F12YS;

```

%LINK 3

```

F23XS = -F32XS;
F23YS = -F32YS;

```

```

g11 = R4Y;
g12 = -R4X;
g21 = -R333Y;
g22 = R333X;

```

```

ot5 = 0;
ot6 = R333X*m3*g-(R33X*F23YS-R33Y*F23XS);

```

```

determinant7 = (g11*g22) - (g12*g21);
F43XS = ((ot5 * g22) - (g12 * ot6)) / determinant7; %N
F43YS = ((g11 * ot6) - (ot5 * g21)) / determinant7; %N
F53XS = -F43XS -F23XS;
F53YS = m3*g-F43YS -F23YS ;

```

%LINK 4

```
F34XS = -F43XS;  
F34YS = -F43YS;
```

```
F14XS = -F34XS;  
F14YS = m4*g-F34YS;
```

%LINK 5

```
F35XS = -F53XS;  
F35YS = -F53YS;
```

```
h11 = R6Y;  
h12 = -R6X;  
h21 = -2*R5Y;  
h22 = 2*R5X;
```

```
ot7 = 0;  
ot8 = R5X*m5*g-(R5X*F35YS-R5Y*F35XS);
```

```
determinant8 = (h11*h22) - (h12*h21);  
F65XS = ((ot7 * h22) - (h12 * ot8)) / determinant8; %N  
F65YS = ((h11 * ot8) - (ot7 * h21)) / determinant8; %N
```

%LINK 6

```
F56XS = -F65XS;  
F56YS = -F65YS;
```

```
F16XS = -F56XS;  
F16YS = m6*g-F56YS;
```

%FP

```
FPXS = -F65XS -F35XS;  
FPYS = m5*g-F65YS -F35YS;  
FPS = sqrt(FPXS^2+FPYS^2);  
FPTANS = FPXS*Ut_X + FPYS*Ut_Y; %Tangent Component of the Force on Point P
```

%UPDATE ALL VECTORS

```
F12XS_all = [F12XS_all,F12XS];  
F12YS_all = [F12YS_all,F12YS];  
F18XS_all = [F18XS_all,F18XS];  
F19XS_all = [F19XS_all,F19XS];  
F28XS_all = [F28XS_all,F28XS];  
F29XS_all = [F29XS_all,F29XS];  
F82XS_all = [F82XS_all,F82XS];  
F92XS_all = [F92XS_all,F92XS];  
F23XS_all = [F23XS_all,F23XS];  
F23YS_all = [F23YS_all,F23YS];  
F34XS_all = [F34XS_all,F34XS];  
F34YS_all = [F34YS_all,F34YS];  
F14XS_all = [F14XS_all,F14XS];  
F14YS_all = [F14YS_all,F14YS];  
F35XS_all = [F35XS_all,F35XS];  
F35YS_all = [F35YS_all,F35YS];  
F56XS_all = [F56XS_all,F56XS];  
F56YS_all = [F56YS_all,F56YS];  
F16XS_all = [F16XS_all,F16XS];  
F16YS_all = [F16YS_all,F16YS];  
FPXS_all = [FPXS_all,FPXS];
```

```

FPYS_all = [FPYS_all,FPYS];
FPS_all = [FPS_all,FPS];
FPS_tanall = [FPS_tanall,FPTANS];

```

%EQUATION OF MOTION

%CHANGE IN KINETIC ENERGY

```

A2 = IG2*1000*(theta_2_prime)^2 + m2;
A3 = IG3*1000*(theta_3_prime)^2 + m3*((RG3x_prime)^2 + (RG3y_prime)^2);
A4 = IG4*1000*(theta_4_prime)^2;
A5 = IG5*1000*(theta_5_prime)^2 + m5*((RG5x_prime)^2 + (RG5y_prime)^2);
A6 = IG6*1000*(theta_6_prime)^2;
Asum = A2 + A3 + A4 + A5 + A6; %Equivalent Mass Moment of Inertia
Asum_all = [Asum_all,Asum]; %

B2 = IG2*theta_2_prime*theta_2_2prime*(1000)^2;
B3 = IG3*theta_3_prime*theta_3_2prime*(1000)^2 + m3*(RG3x_prime*RG3x_2prime +
RG3y_prime*RG3y_2prime)*1000;
B4 = IG4*theta_4_prime*theta_4_2prime*(1000)^2;
B5 = IG5*theta_5_prime*theta_5_2prime*(1000)^2 + m5*(RG5x_prime*RG5x_2prime +
RG5y_prime*RG5y_2prime)*1000;
B6 = IG6*theta_6_prime*theta_6_2prime*(1000)^2;
Bsum = B2 + B3 + B4 + B5 + B6;

```

```
Ttot = Asum*R_doubledot_22 + Bsum*(r_dot/1000)^2;
```

%CHANGE IN POTENTIAL ENERGY

```

Us = k * ((R11-R22)-Rs)/1000; %N
Ug = m3*g*RG3y_prime + m5*g*RG5y_prime;
Utot = Us + Ug;

```

%WORK DUE TO EXTERNAL FORCES

```
Wf = F12X*1;
```

%POWER EQUATION

```
P = Ttot + Utot + Wf;
```

%TANGENT FORCE

```
Fp_power_tan = (T12*(theta_2_prime)-P) / Rp_prime;
```

%PERCENT CONTRIBUTION

```

T_perc = abs(Ttot)/(abs(Ttot) + abs(Ug) + abs(Us) + abs(Wf));
U_perc = abs(Utot)/(abs(Ttot) + abs(Ug) + abs(Us) + abs(Wf));
Wf_perc = abs(Wf)/(abs(Ttot) + abs(Ug) + abs(Us) + abs(Wf));

```

%UPDATE VECTOR

```

Fp_power_tan_all = [Fp_power_tan_all,Fp_power_tan];
end

```

```

%%TABULATED VALUES%%%%%%%%%%%%%%%%%%%%%%%%%%%%%%%%%%%%%%%%%%%%%%%%%%%%%%%%%%%%%%%%%%%%%%%%
%%DYNAMIC%%%%%%%%%%%%%%%%%%%%%%%%%%%%%%%%%%%%%%%%%%%%%%%%%%%%%%%%%%%%%%%%%%%%%%%%
fprintf('R22:  Actuator Force:  Spring Force:\n')
fprintf('mm  N  N\n')
for x = 1:25:751
fprintf('%6.2f %6.2f %6.2f \n',R22all(x),F19X_all(x),F18X_all(x));
end

```

```

fprintf('\n')

fprintf(' R22:   F12X:   F12Y:   F23X:   F23Y:\n')
fprintf(' mm   N   N   N   N\n')
for x = 1:25:751
    fprintf('%5.1f %6.0f %6.0f %6.2f %6.2f \n',R22all(x),F12X_all(x),F12Y_all(x),F23X_all(x),F23Y_all(x));
end

fprintf('\n')

fprintf(' R22:   F16X:   F16Y:   F56X:   F56Y:\n')
fprintf(' (mm)   (N)   (N)   (N)   (N) \n')
for x = 1:25:751
    fprintf('%5.1f%9.2f%9.2f%10.2f%8.2f \n',R22all(x),F16X_all(x),F16Y_all(x),F56X_all(x),F56Y_all(x));
end

fprintf('\n')

fprintf(' R22:   F43X:   F43Y:   F53X:   F53Y: \n')
fprintf(' (mm)   (N)   (N)   (N)   (N) \n')
for x = 1:25:751
    fprintf('%5.1f%9.2f%9.2f%10.2f%10.2f \n',R22all(x),-F34X_all(x),-F34Y_all(x),-F35X_all(x),-F35Y_all(x));
end

fprintf('\n')

fprintf(' R22:   F14X:   F14Y:   FPX:   FPY: FP(tangential): \n')
fprintf(' (mm)   (N)   (N)   (N)   (N)   (N)\n')
for x = 1:25:751
    fprintf('%5.1f%10.2f%10.2f%10.2f%10.2f%10.2f \n',R22all(x),F14X_all(x),F14Y_all(x),FPX_all(x),FPY_all(x),Fp_tanall(x));
end

%%%%%%%%%%%%%%%%%%%%%%%%%%%%%%%%%%%%%%%%%%%%%%%%%%%%%%%%%%%%%%%%%%%%%%%%%%
fprintf('\n')

fprintf('R22:   Actuator Force:   Spring Force:\n')
fprintf('mm   N   N\n')
for x = 1:25:751
    fprintf('%5.1f %6.2f %6.2f \n',R22all(x),F19XS_all(x),F18XS_all(x));
end

fprintf('\n')

fprintf(' R22:   F12X:   F12Y:   F23X:   F23Y:\n')
fprintf(' mm   N   N   N   N\n')
for x = 1:25:751
    fprintf('%5.1f %6.0f %6.0f %6.2f %6.2f \n',R22all(x),F12XS_all(x),F12YS_all(x),F23XS_all(x),F23YS_all(x));
end

fprintf('\n')

fprintf(' R22:   F16X:   F16Y:   F56X:   F56Y:\n')
fprintf(' (mm)   (N)   (N)   (N)   (N) \n')

```



```

for x = 1:25:751
    fprintf( '%5.1f%9.2f%9.2f%10.2f%8.2f \n',R22all(x),F16XS_all(x),F16YS_all(x),F56XS_all(x),F56YS_all(x));
end

fprintf( '\n')

fprintf( ' R22:   F43X:   F43Y:   F53X:   F53Y:   \n')
fprintf( ' (mm)   (N)     (N)     (N)     (N)     \n')
for x = 1:25:751
    fprintf( '%5.1f%9.2f%9.2f%10.2f%10.2f \n',R22all(x),-F34XS_all(x),-F34YS_all(x),-F35XS_all(x),-F35YS_all(x));
end

fprintf( '\n')

fprintf( ' R22:   F14X:   F14Y:   FPX:   FPY: FP(tangential): \n')
fprintf( ' (mm)   (N)     (N)     (N)     (N)     (N)\n')
for x = 1:25:751
    fprintf( '%5.1f%10.2f%10.2f%10.2f%10.2f%10.2f \n',R22all(x),F14XS_all(x),F14YS_all(x),FPXS_all(x),FPYS_all(x),FPS_tanall(x));
end
%%%%%%%%%%%%%%%%%%%%%%%%%%%%%%%%%%%%%%%%%%%%%%%%%%%%%%%%%%%%%%%%%%%%%%%%%%%%%%
%EQUATION OF MOTION%%%%%%%%%%%%%%%%%%%%%%%%%%%%%%%%%%%%%%%%%%%%%%%%%%%%%%%%%%%%%%%%%%%%%%%%%%%%%%
fprintf( '\n')

fprintf( ' R22:   Equivalent Mass Moment of Inertia:\n')
fprintf( ' (mm)                               kg\n')
for x = 1:25:751
    fprintf( '%5.1f           %10.2f \n',R22all(x),Asum_all(x));
end

%%%%%%%%%%%%%%%%%%%%%%%%%%%%%%%%%%%%%%%%%%%%%%%%%%%%%%%%%%%%%%%%%%%%%%%%%%%%%%
%PLOTS%%%%%%%%%%%%%%%%%%%%%%%%%%%%%%%%%%%%%%%%%%%%%%%%%%%%%%%%%%%%%%%%%%%%%%%%%%%%%%
%DYNAMIC%%%%%%%%%%%%%%%%%%%%%%%%%%%%%%%%%%%%%%%%%%%%%%%%%%%%%%%%%%%%%%%%%%%%%%%%%%%%%%
%PLOT ACTUATOR FORCE AGAINST THE INPUT POSITION OF R22
figure
plot(R22all,F19X_all)
xlabel('Length of Input Link - R22 (mms)')
ylabel('Actuator Force (N)')
title('Actuator Force vs. Length of Input Link')

%PLOT SPRING FORCE AGAINST THE INPUT POSITION OF R22
figure
plot(R22all,F18X_all)
xlabel('Length of Input Link - R22 (mms)')
ylabel('Spring Force (N)')
title('Spring Force vs. Length of Input Link')

%PLOT F12
figure
plot(R22all,F12X_all,R22all,F12Y_all)
xlabel('Length of Input Link - R22 (mms)')
ylabel('Force (N)')
legend('F12X','F12Y')
title('X and Y components of F12 Reaction Force')

%PLOT F32
figure
plot(R22all,-F23X_all,R22all,-F23Y_all)

```

```
xlabel('Length of Input Link - R22 (mms)')
ylabel('Force (N)')
legend('F32X', 'F32Y')
title('X and Y components of F32 Reaction Force')
```

```
%PLOT F34
figure
plot(R22all, F34X_all, R22all, F34Y_all)
xlabel('Length of Input Link - R22 (mms)')
ylabel('Force (N)')
ylim([0 15000])
legend('F34X', 'F34Y')
title('X and Y components of F34 Reaction Force')
```

```
%PLOT F14
figure
plot(R22all, F14X_all, R22all, F14Y_all)
xlabel('Length of Input Link - R22 (mms)')
ylabel('Force (N)')
legend('F14X', 'F14Y')
title('X and Y components of F14 Reaction Force')
```

```
%PLOT F35
figure
plot(R22all, F35X_all, R22all, F35Y_all)
xlabel('Length of Input Link - R22 (mms)')
ylabel('Force (N)')
legend('F35X', 'F35Y')
title('X and Y components of F35 Reaction Force')
```

```
%PLOT F56
figure
plot(R22all, F56X_all, R22all, F56Y_all)
xlabel('Length of Input Link - R22 (mms)')
ylabel('Force (N)')
legend('F56X', 'F56Y')
title('X and Y components of F56 Reaction Force')
```

```
%PLOT F16
figure
plot(R22all, F16X_all, R22all, F16Y_all)
xlabel('Length of Input Link - R22 (mms)')
ylabel('Force (N)')
legend('F16X', 'F16Y')
title('X and Y components of F16 Reaction Force')
```

```
%PLOT FP
figure
plot(R22all, FPX_all, R22all, FPY_all)
xlabel('Length of Input Link - R22 (mms)')
ylabel('Force (N)')
legend('FPX', 'FPY')
title('X and Y components of FP External Force')
```

```
%PLOT FP TAN
figure
plot(R22all, Fp_tanall)
xlabel('Length of Input Link - R22 (mms)')
```

```
ylabel('Force (N)')
title('Tangent component of FP External Force')
```

%%%

%STATIC: PLOT ACTUATOR FORCE AGAINST THE INPUT POSITION OF R22

```
figure
plot(R22all,F19X_all)
xlabel('Length of Input Link - R22 (mms)')
ylabel('Actuator Force (N)')
title('Static: Actuator Force vs. Length of Input Link')
```

%PLOT SPRING FORCE AGAINST THE INPUT POSITION OF R22

```
figure
plot(R22all,F18X_all)
xlabel('Length of Input Link - R22 (mms)')
ylabel('Spring Force (N)')
title('Static: Spring Force vs. Length of Input Link')
```

%PLOT F12S AGAINST THE INPUT POSITION OF R22

```
figure
plot(R22all,F12XS_all, R22all,F12YS_all)
xlabel('Length of Input Link - R22 (mms)')
ylabel('Force (N)')
legend('F12X','F12Y')
title('Static: F12 vs. Length of Input Link')
```

%PLOT F14S

```
figure
plot(R22all,F14XS_all,R22all,F14YS_all)
xlabel('Length of Input Link - R22 (mms)')
ylabel('Force (N)')
legend('F14X','F14Y')
title('Static: X and Y components of F14 Reaction Force')
```

%PLOT F16S

```
figure
plot(R22all,F16XS_all,R22all,F16YS_all)
xlabel('Length of Input Link - R22 (mms)')
ylabel('Force (N)')
legend('F16X','F16Y')
title('Static: X and Y components of F16 Reaction Force')
```

%PLOT F32S

```
figure
plot(R22all,-F23XS_all,R22all,-F23YS_all)
xlabel('Length of Input Link - R22 (mms)')
ylabel('Force (N)')
legend('F32X','F32Y')
title('Static: X and Y components of F32 Reaction Force')
```

%PLOT F23S

```
figure
plot(R22all,F23XS_all,R22all,F23YS_all)
xlabel('Length of Input Link - R22 (mms)')
ylabel('Force (N)')
legend('F23X','F23Y')
title('Static: X and Y components of F23 Reaction Force')
```

```
%PLOT F34S
figure
plot(R22all,F34XS_all,R22all,F34YS_all)
xlabel('Length of Input Link - R22 (mms)')
ylabel('Force (N)')
ylim([0 15000])
legend('F34X','F34Y')
title('Static: X and Y components of F34 Reaction Force')
```

```
%PLOT F43S
figure
plot(R22all,-F34XS_all,R22all,-F34YS_all)
xlabel('Length of Input Link - R22 (mms)')
ylabel('Force (N)')
ylim([-15000 0])
legend('F43X','F43Y')
title('Static: X and Y components of F43 Reaction Force')
```

```
%PLOT F53S
figure
plot(R22all,-F35XS_all,R22all,-F35YS_all)
xlabel('Length of Input Link - R22 (mms)')
ylabel('Force (N)')
legend('F53X','F53Y')
title('Static: X and Y components of F53 Reaction Force')
```

```
%PLOT F35S
figure
plot(R22all,F35XS_all,R22all,F35YS_all)
xlabel('Length of Input Link - R22 (mms)')
ylabel('Force (N)')
legend('F35X','F35Y')
title('Static: X and Y components of F35 Reaction Force')
```

```
%PLOT F56S
figure
plot(R22all,F56XS_all,R22all,F56YS_all)
xlabel('Length of Input Link - R22 (mms)')
ylabel('Force (N)')
legend('F56X','F56Y')
title('Static: X and Y components of F56 Reaction Force')
```

```
%PLOT F65S
figure
plot(R22all,-F56XS_all,R22all,-F56YS_all)
xlabel('Length of Input Link - R22 (mms)')
ylabel('Force (N)')
legend('F65X','F65Y')
title('Static: X and Y components of F65 Reaction Force')
```

```
%PLOT FPXS AND FPYS
figure
plot(R22all,FPXS_all,R22all,FPYS_all)
xlabel('Length of Input Link - R22 (mms)')
ylabel('Force (N)')
legend('FPX','FPY')
title('Static: X and Y components of FP Reaction Force')
```

```
%PLOT FPS
figure
plot(R22all,FPS_all)
xlabel('Length of Input Link - R22 (mms)')
ylabel('Point P Force (N)')
title('Static: Force at Point P vs. Length of Input Link')
```

```
%PLOT TANGENT OF FPS
figure
plot(R22all,FPS_tanall)
xlabel('Length of Input Link - R22 (mms)')
ylabel('Tangent Force of Point P (N)')
title('Static: Tangent Force at Point P vs. Length of Input Link')
```

```
%%%%%%%%EQUATION OF MOTION%%%%%%%%
%PLOT TANGENT OF FP FROM EOM
figure
plot(R22all,Fp_power_tan_all)
xlabel('Length of Input Link - R22 (mms)')
ylabel('Tangent Force of Point P (N)')
title('EOM: Tangent Force at Point P vs. Length of Input Link')
```